NGC7727: Numerical model of Supermassive Black Holes and host galaxy complex co-evolution.

VolkswagenStiftung

2020-2021-2022
2023

JÜLICH Forschungszentrum | JÜLICH SUPERCOMPUTING CENTRE

NRFU

2020-2021-~~2022~~
2023

<u>Dr. Sci. Peter Berczik</u>

Dr. M. Ishchenko, M. Sobolenko
MAO National Academy of Sciences of Ukraine Kiev

Dr. K. Voggel, Dr. C. Boily
Astronomical Observatory Strasbourg University, France

2023 August 28.

BH's in galaxies (MW - Sgr A*)

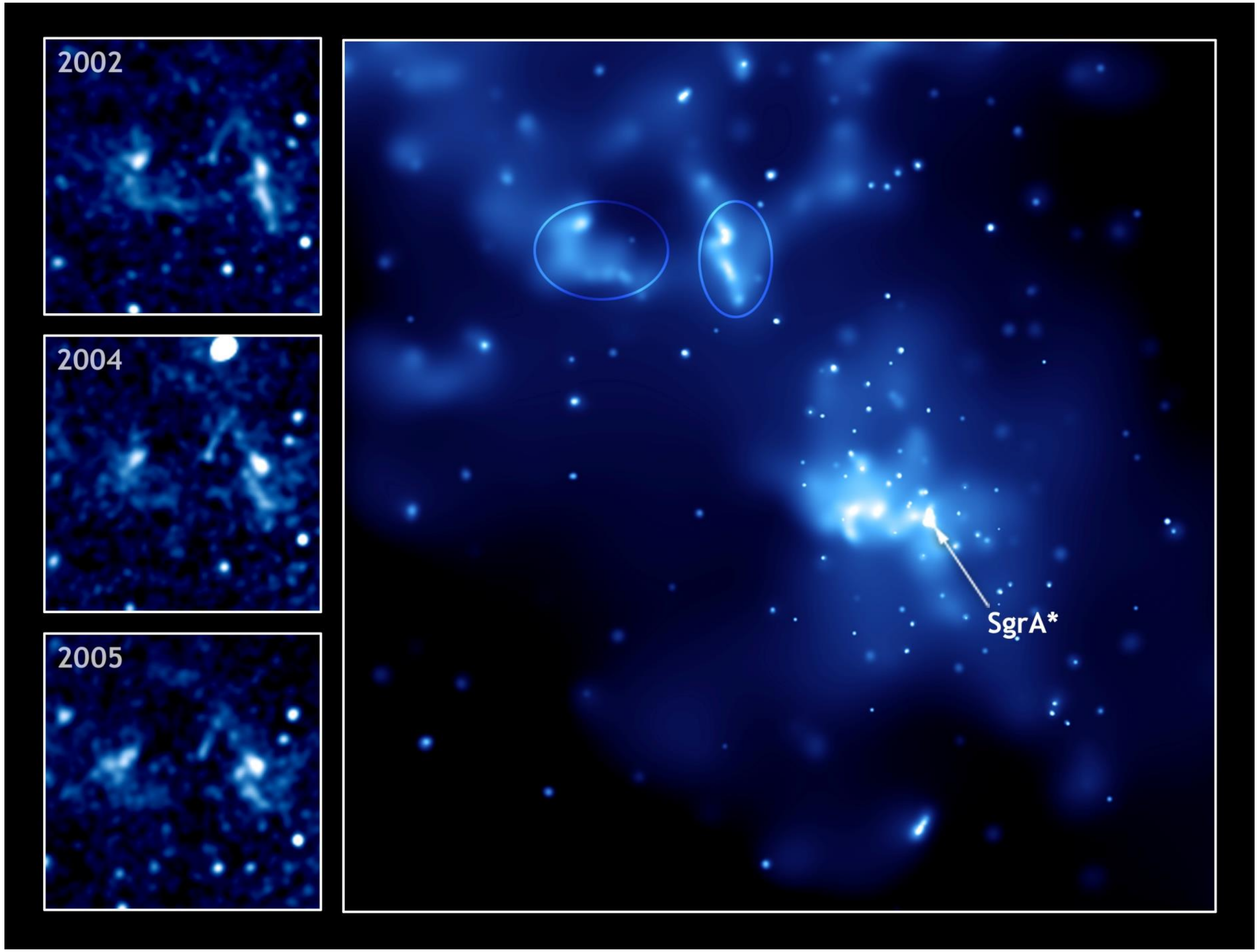

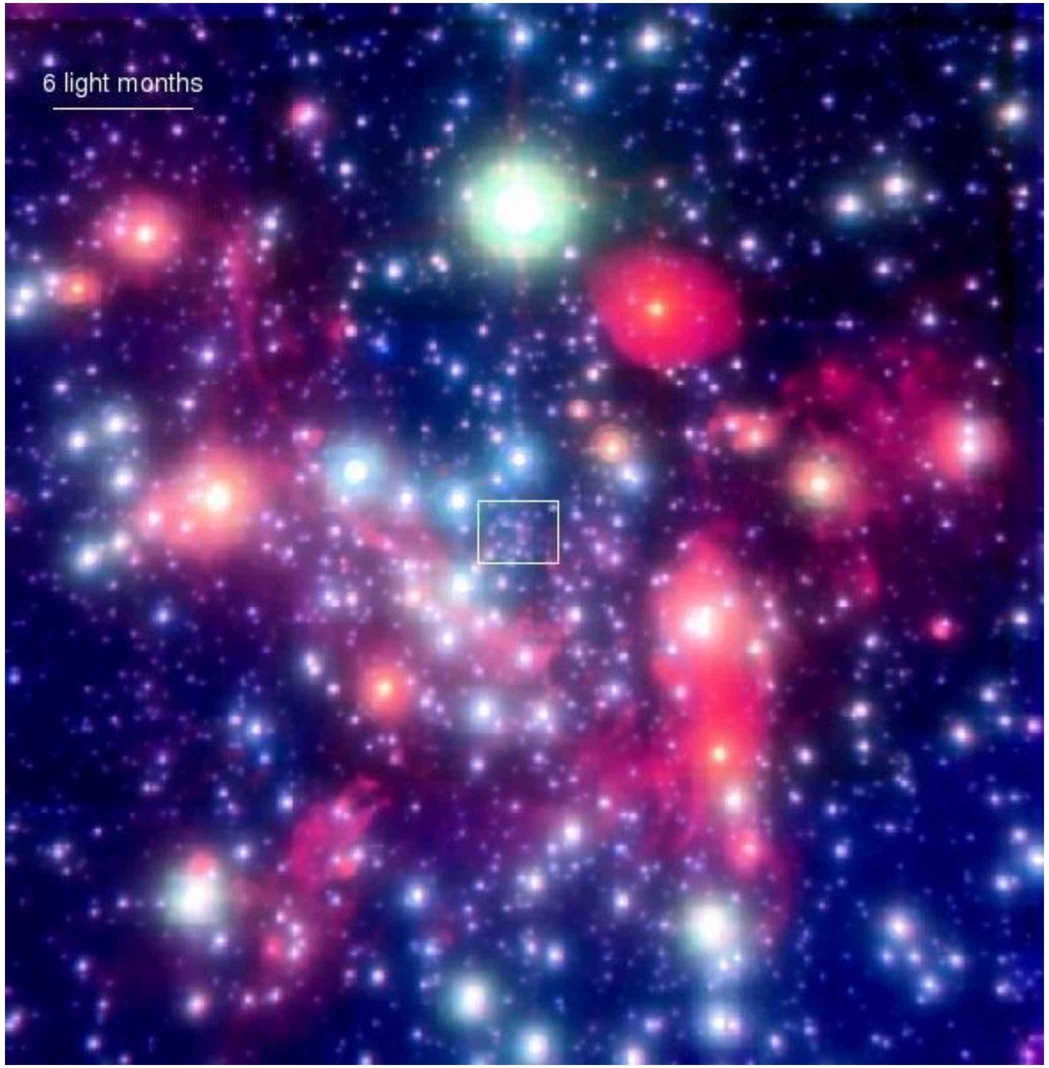

BH’s in galaxies (MW - Sgr A*)

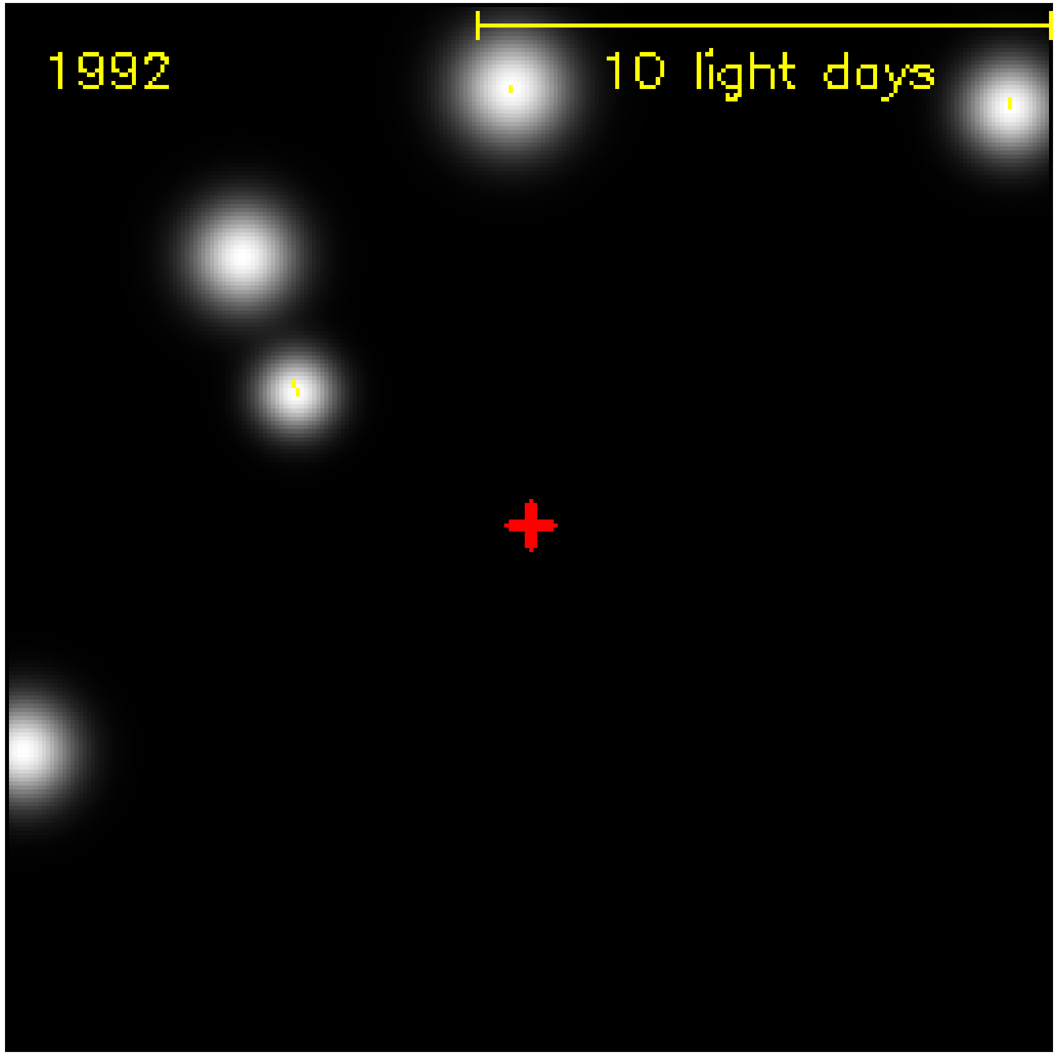

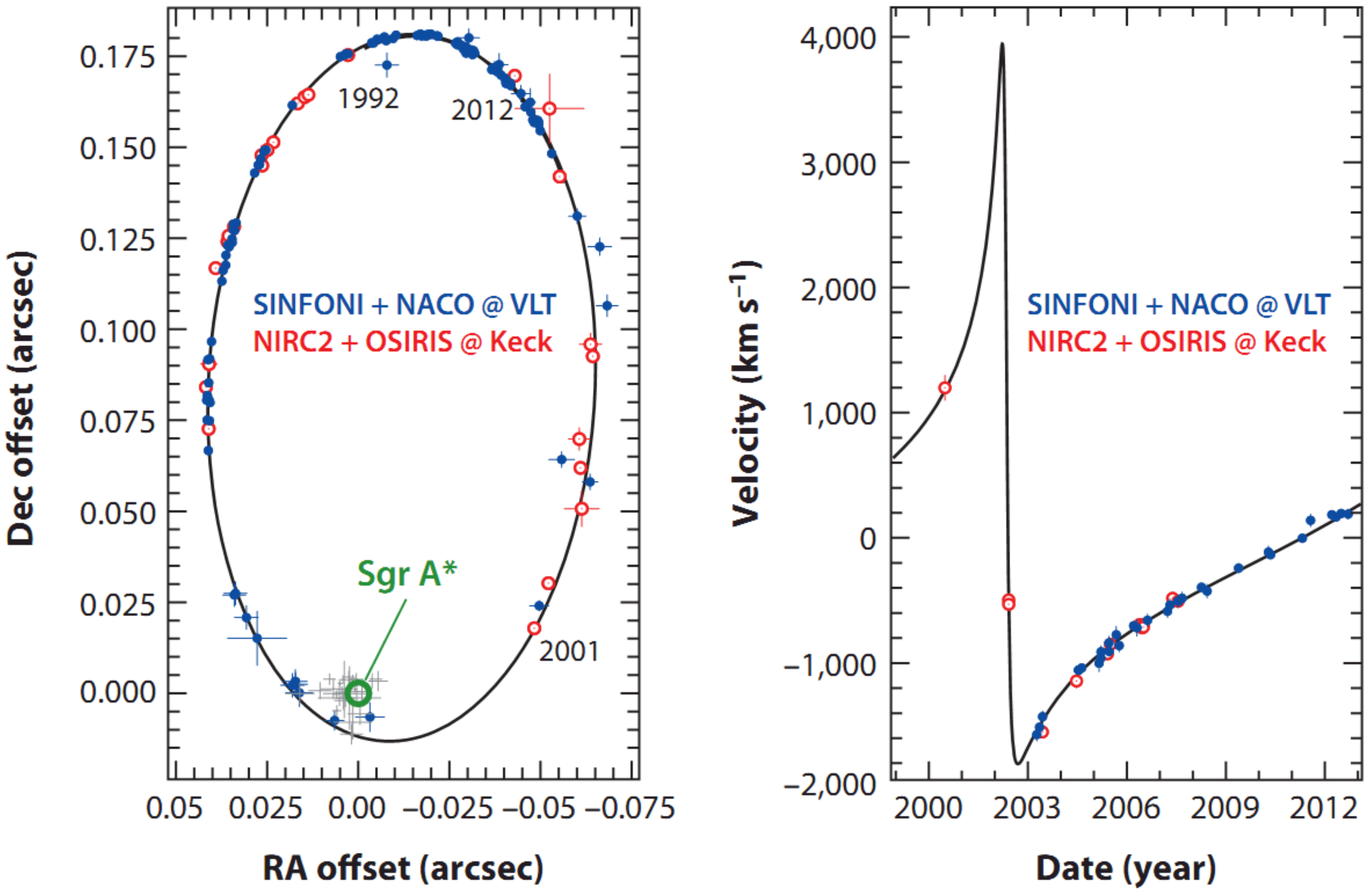

BH's in galaxies (MW - Sgr A*)

The Nobel Prize in Physics 2020

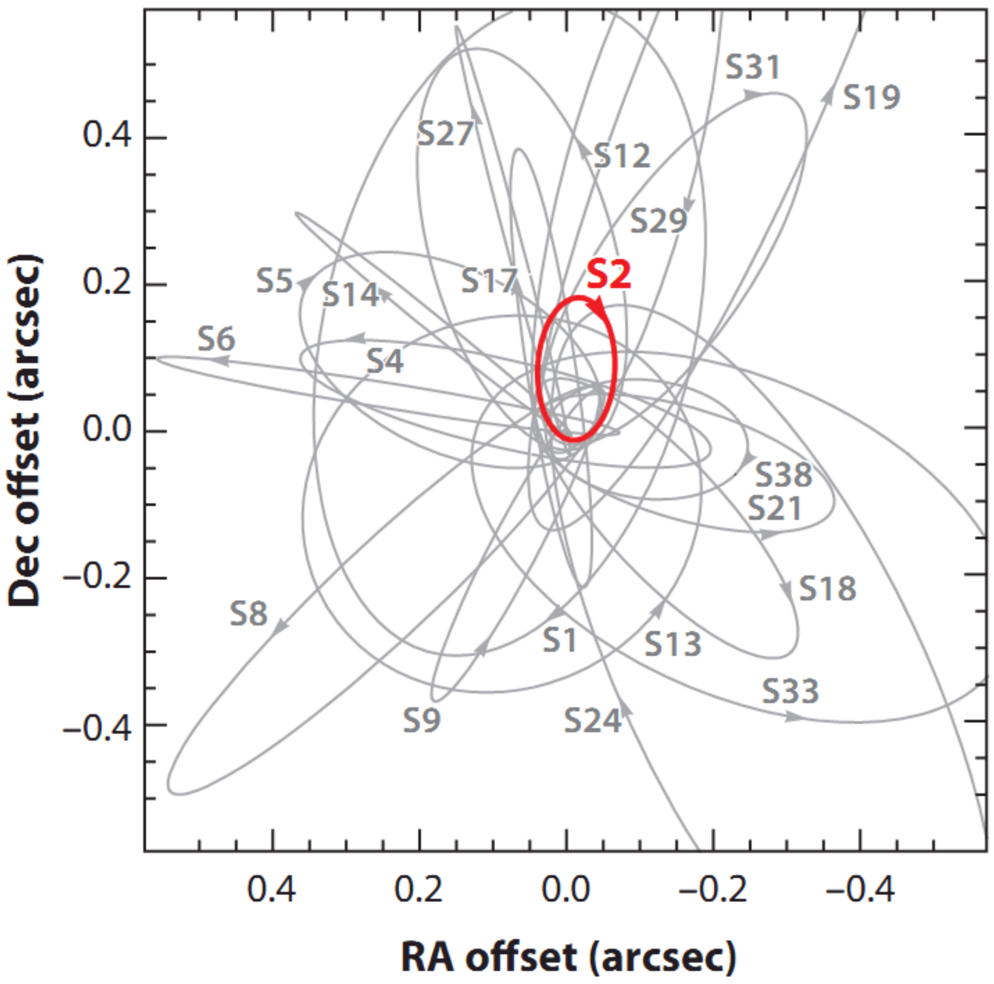

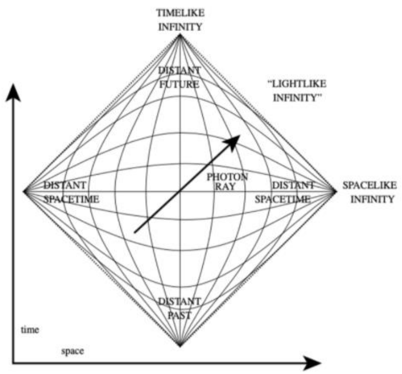

$$M_\bullet = 4.30 \pm 0.20(\mathrm{stat}) \pm 0.30(\mathrm{sys}) \times 10^6\ \mathrm{M}_\odot$$
$$R_0 = 8.28(\pm 0.15)_{\mathrm{stat}}(\pm 0.29)_{\mathrm{sys}}\ \mathrm{kpc}$$
$$\rho_\bullet > 10^{19.5}\ \mathrm{M}_\odot\ \mathrm{pc}^{-3}$$
$$M_{\mathrm{extended}}/M_\bullet < \text{a few} \times 10^{-2}$$

L-R: Roger Penrose, Reinhard Genzel, Andrea Ghez

BH's in galaxies

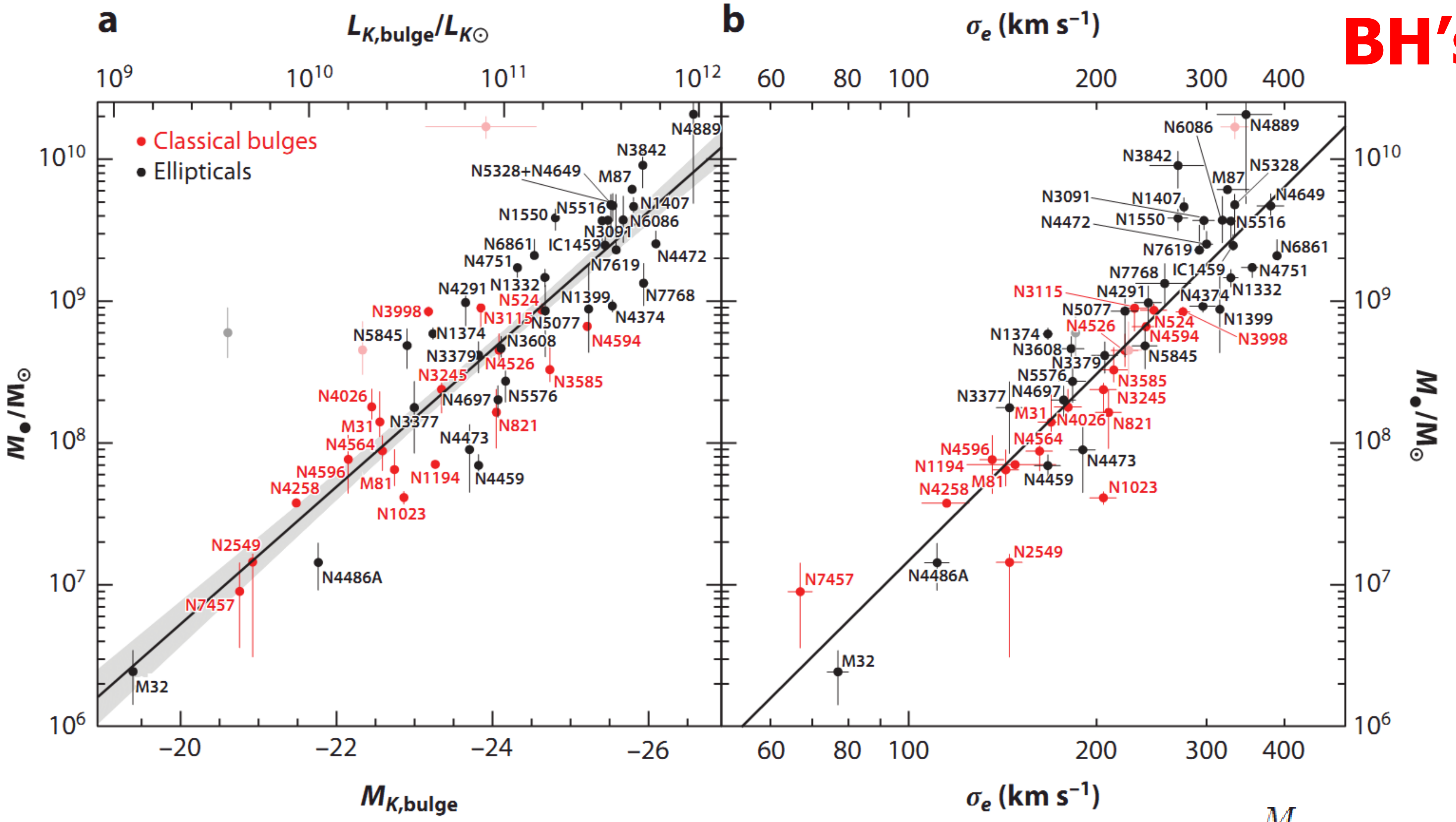

John Kormendy and Luis C. Ho,
Annu. Rev. Astron. Astrophys. 2013. 51:511–653

$$\frac{M_\bullet}{10^9\,\mathrm{M}_\odot} = \left(0.544^{+0.067}_{-0.059}\right)\left(\frac{L_{K,\mathrm{bulge}}}{10^{11}\,L_{K\odot}}\right)^{1.22\pm0.08},$$

$$\frac{M_\bullet}{10^9\,\mathrm{M}_\odot} = \left(0.310^{+0.037}_{-0.033}\right)\left(\frac{\sigma}{200\ \mathrm{km\,s^{-1}}}\right)^{4.38\pm0.29}.$$

Galaxy Collisions ≈ BH's collisions

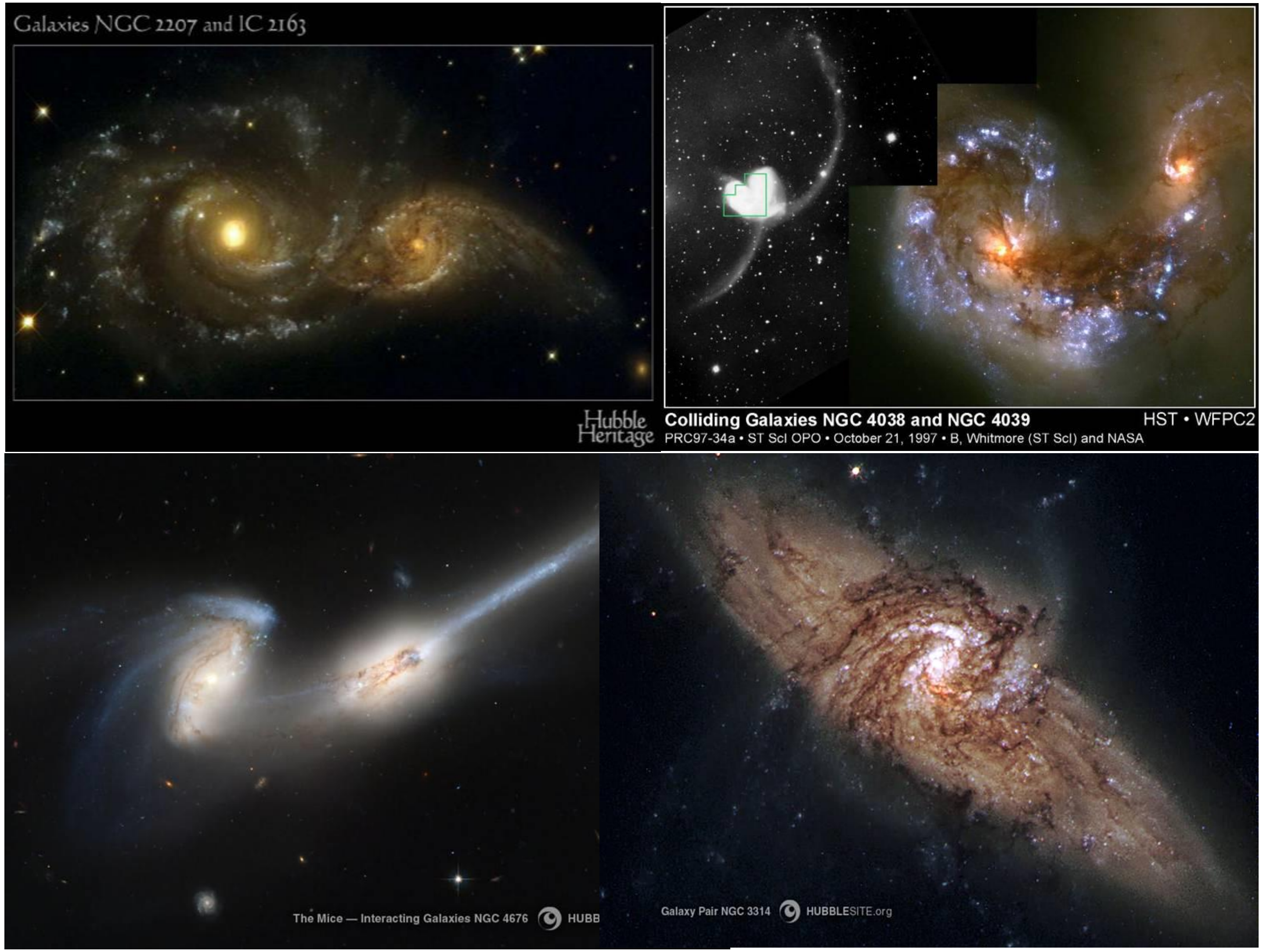

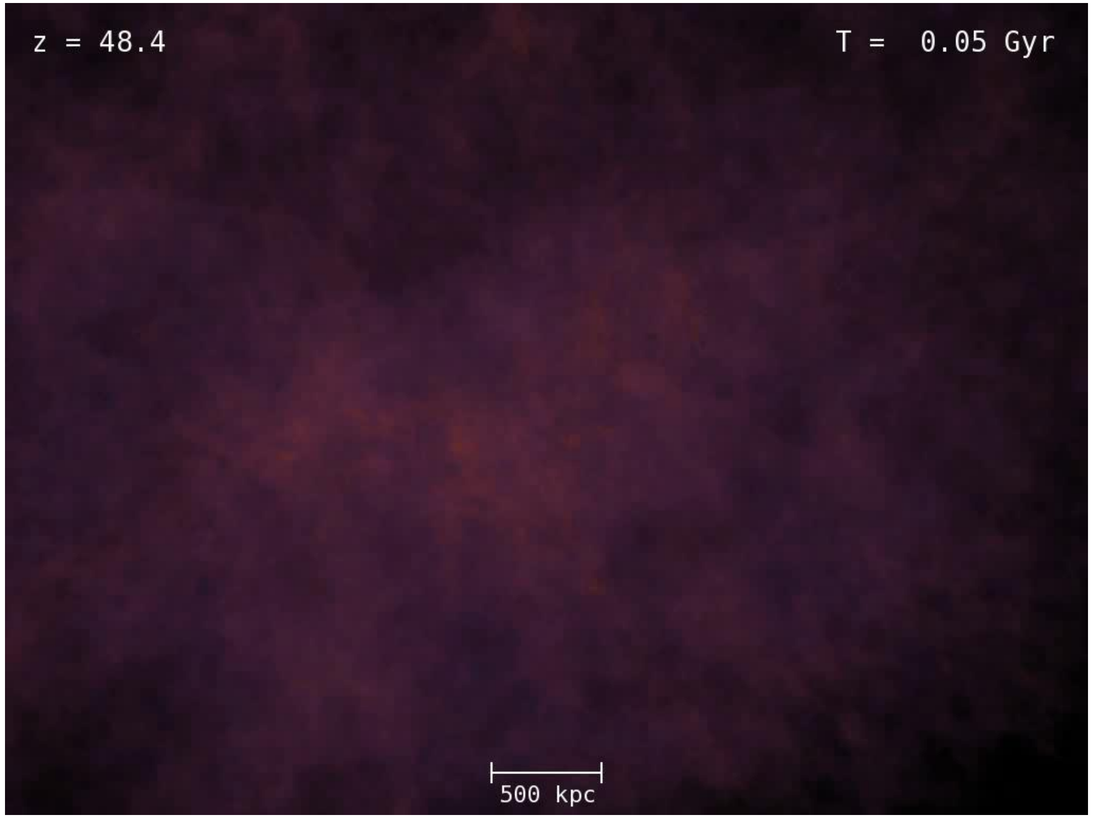

Galaxy Collisions ≈ BH's collisions

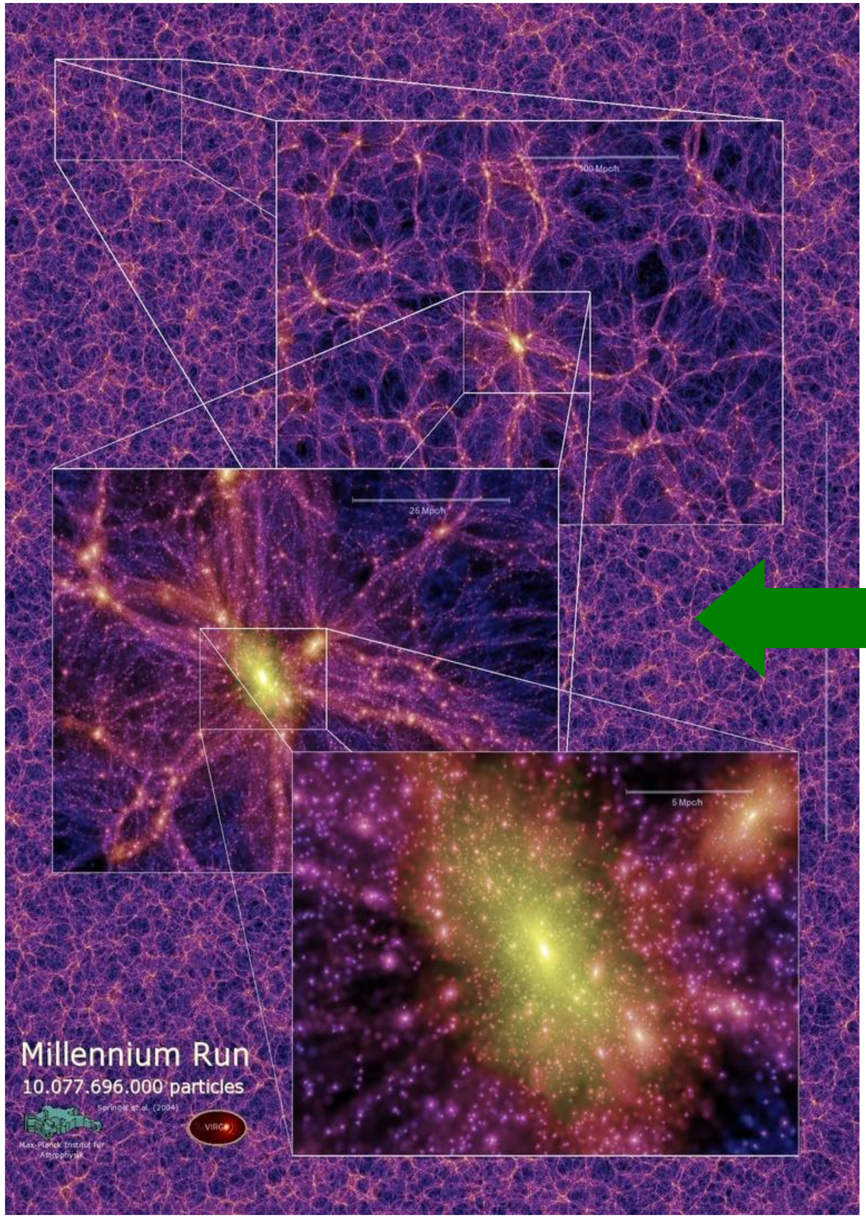

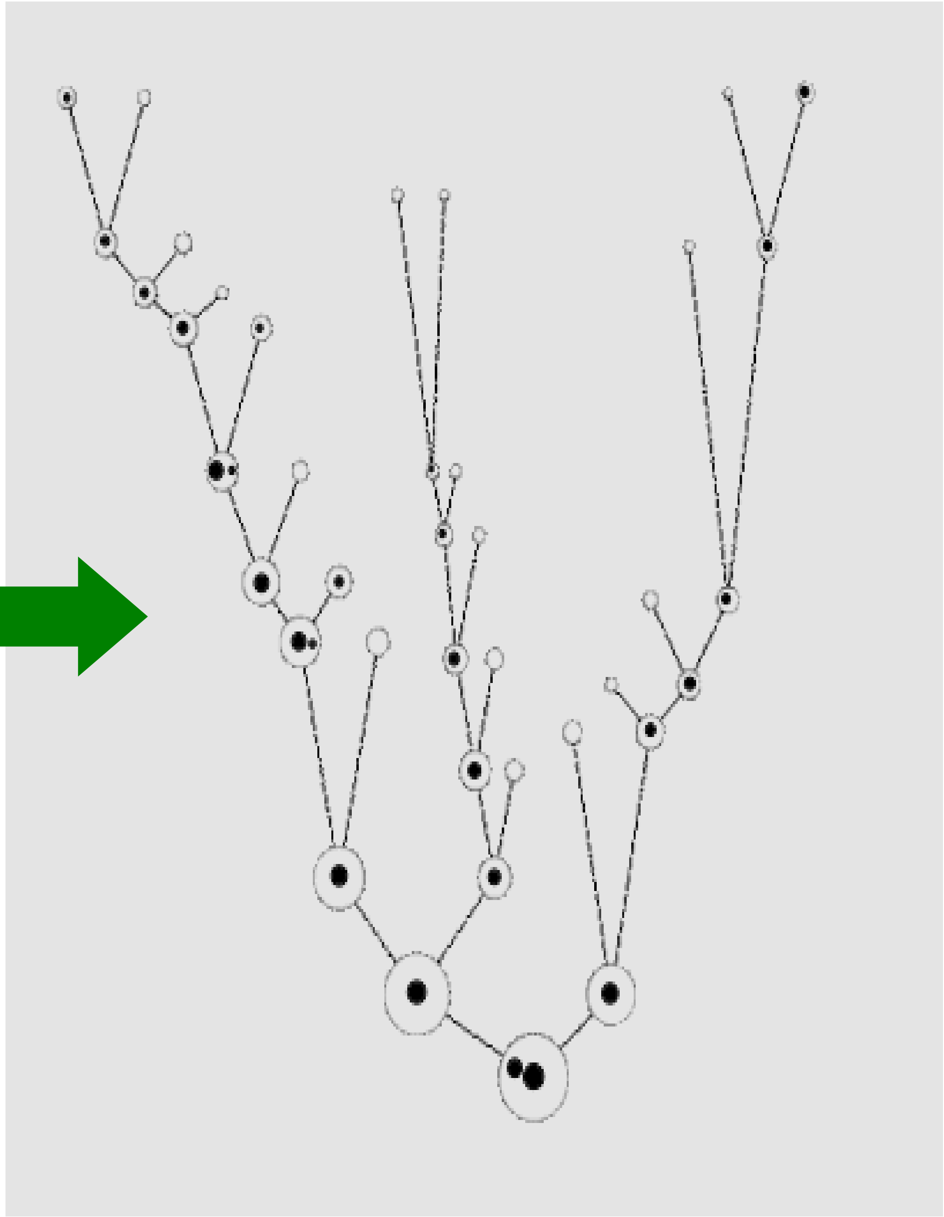

https://www.tng-project.org

-The TNG Collaboration

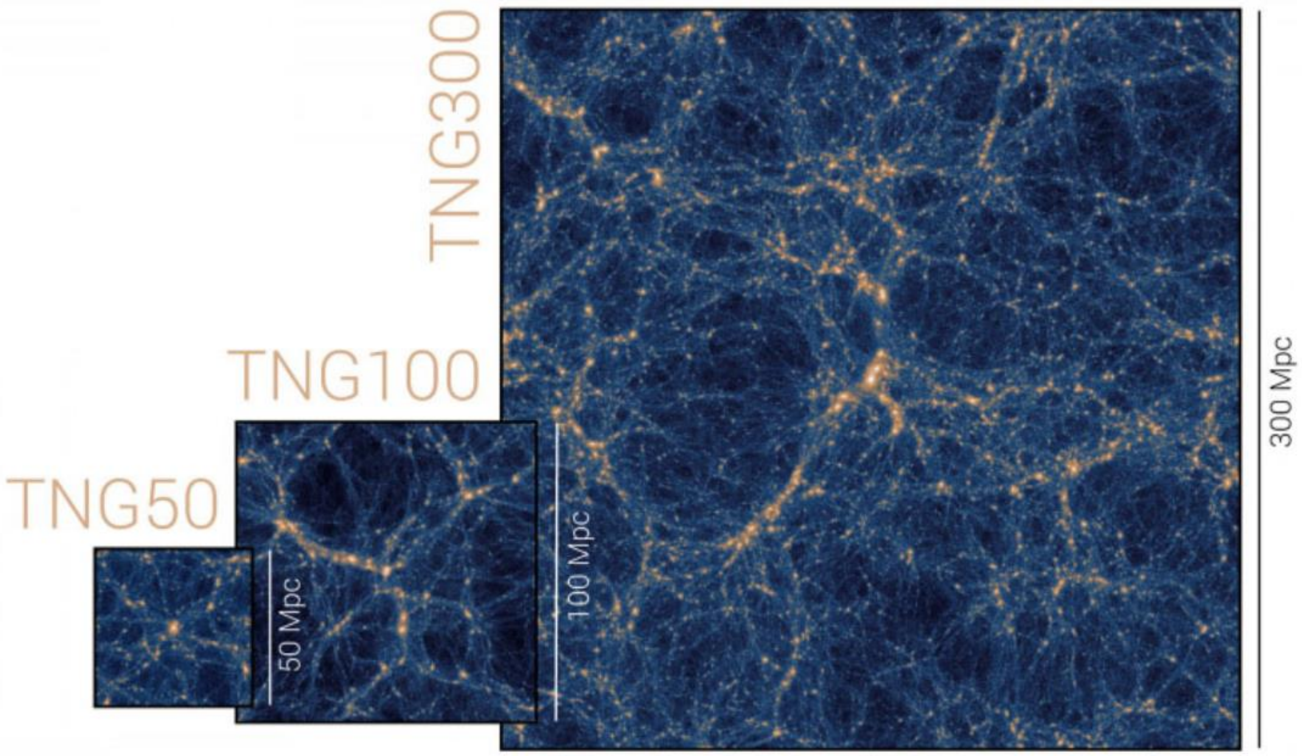

		TNG50	TNG100	TNG300
Volume	[Mpc^3]	51.7^3	110.7^3	302.6^3
L_{box}	[Mpc/h]	35	75	205
N_{GAS}	-	2160^3	1820^3	2500^3
N_{DM}	-	2160^3	1820^3	2500^3
N_{TR}	-	2160^3	2×1820^3	2500^3
m_{baryon}	[$M_\odot$]	8.5×10^4	1.4×10^6	1.1×10^7
m_{DM}	[$M_\odot$]	4.5×10^5	7.5×10^6	5.9×10^7
$\epsilon_{gas,min}$	[pc]	74	185	370
$\epsilon_{DM,\star}$	[pc]	288	740	1480

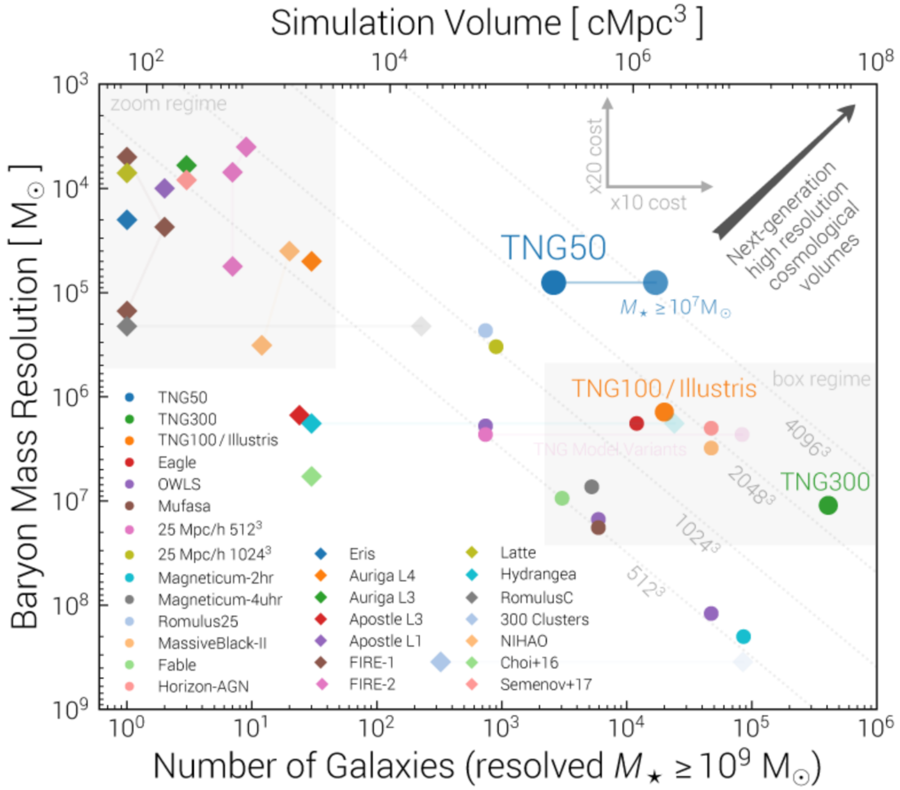

Volker Springel
Heidelberg Institute for Theoretical Studies ➡ MPA
PI: Overall TNG Project

Lars Hernquist
Harvard University

https://www.tng-project.org

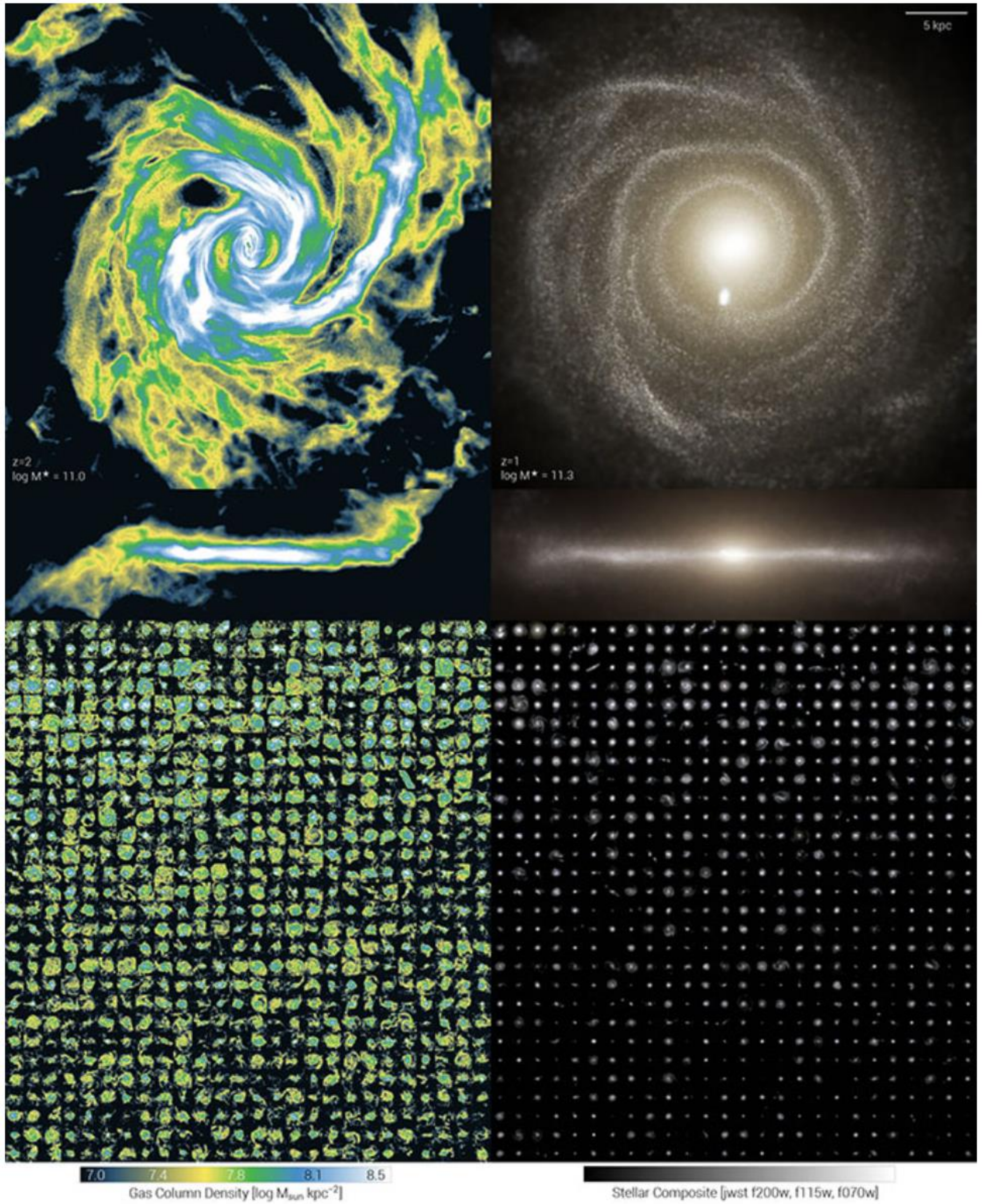

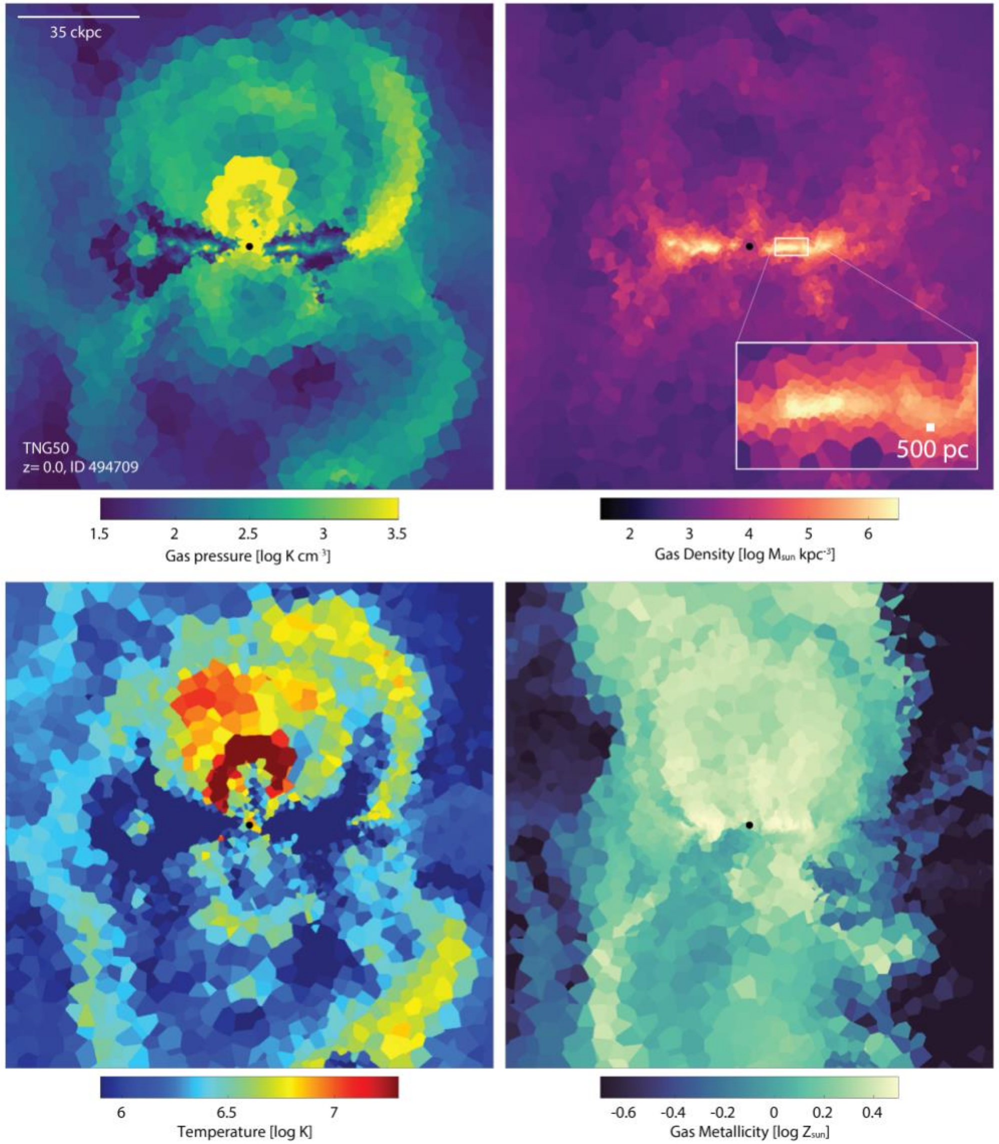

The gaseous (left) and stellar (right) structure of TNG50 galaxies at high redshift. The top shows a massive disk galaxy at z=2 and a descendant at z=1, while the bottom montage reveals ~750 central galaxies at redshift two, from large ellipticals at the center of galaxy groups to smaller, dwarf systems. [large] [ref]

A outflow-driven "bubble" produced by supermassive black hole feedback, around a disky galaxy similar to our own Milky Way at redshift zero, found within the TNG50 simulation. This structure is similar to those observed in gamma-rays by the Fermi telescope, and in x-rays by the eROSITA mission, in our own Galaxy. [large] [ref]

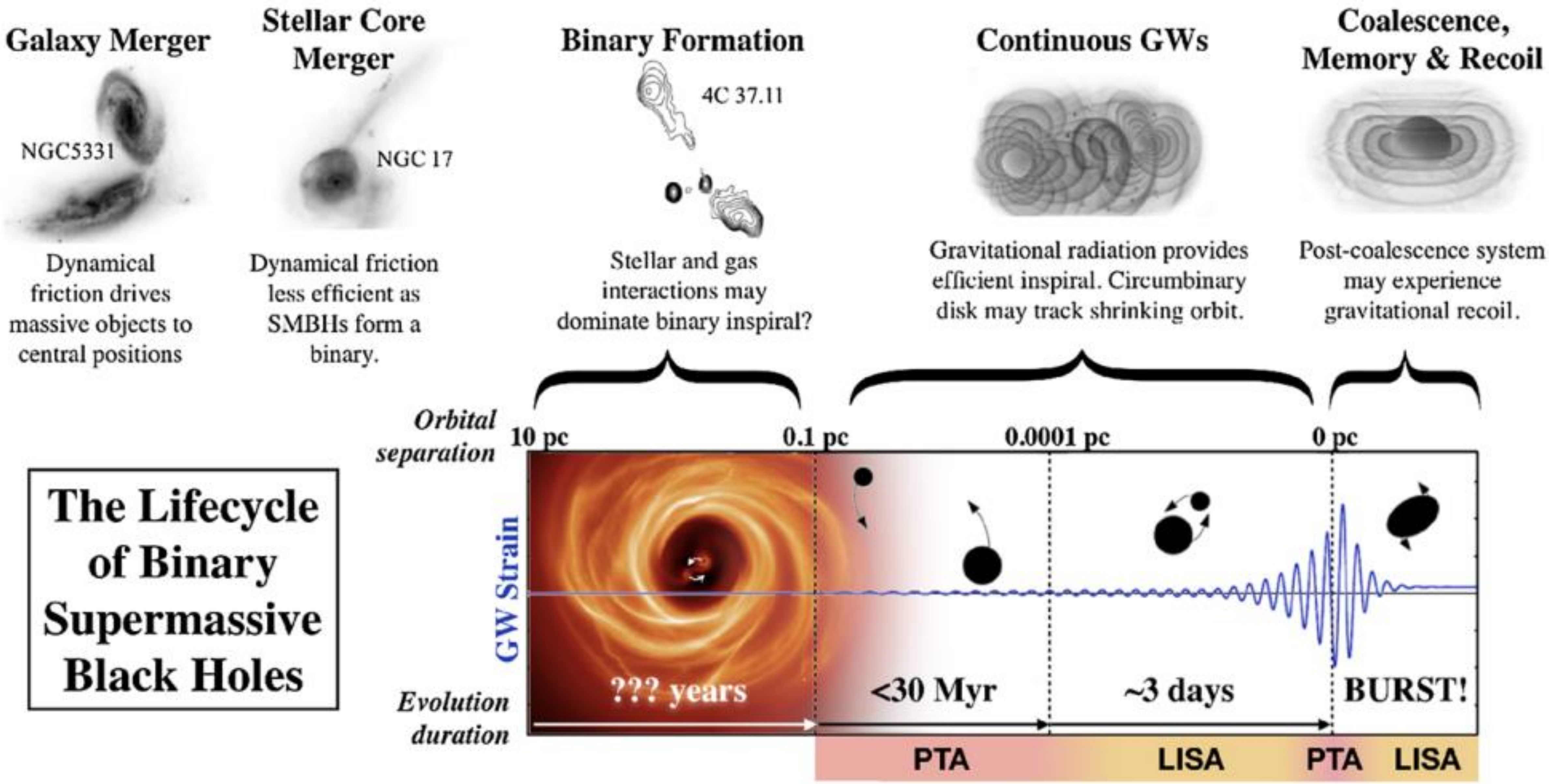

Slide from Margarita

Galaxy Collisions ≈ BH's collisions

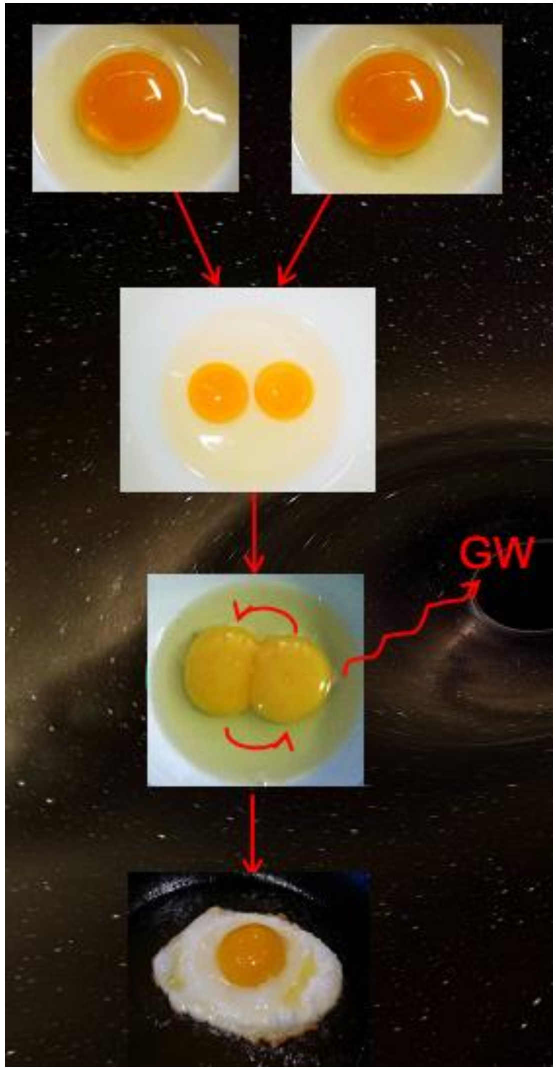

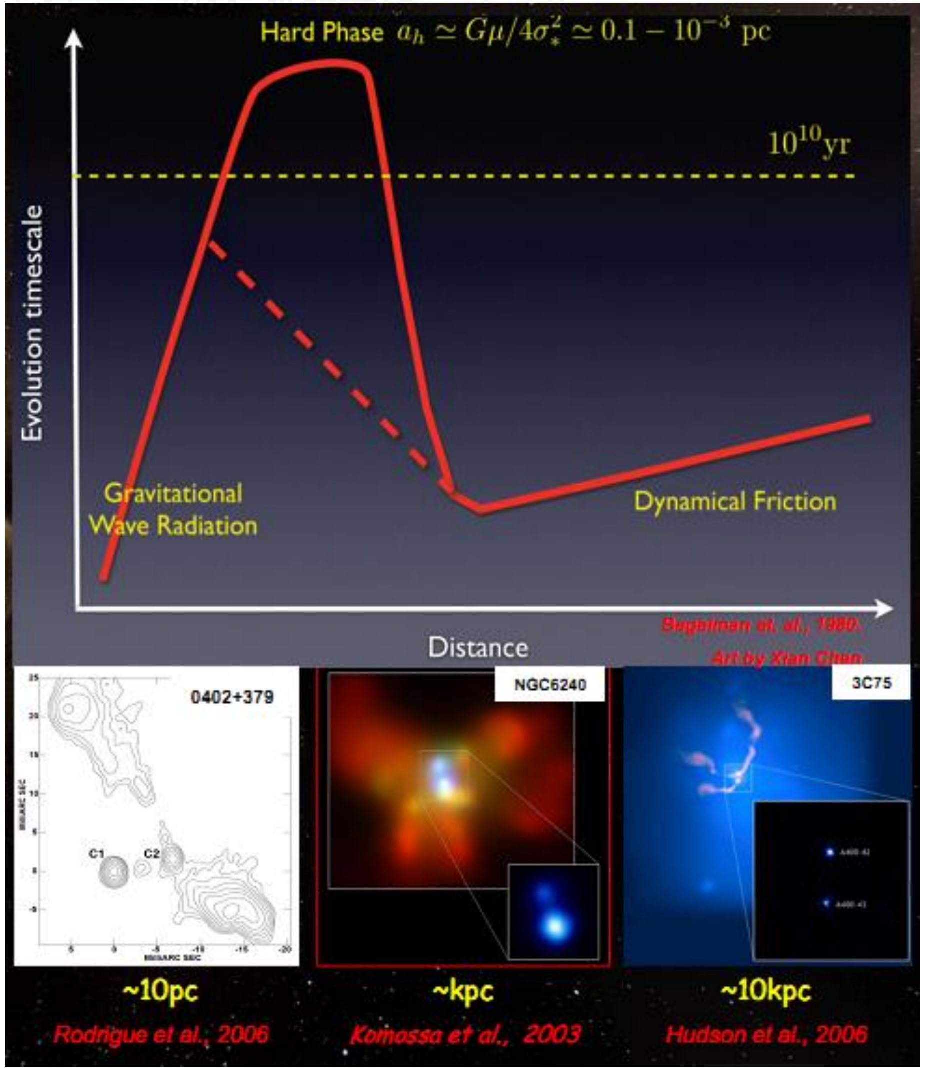

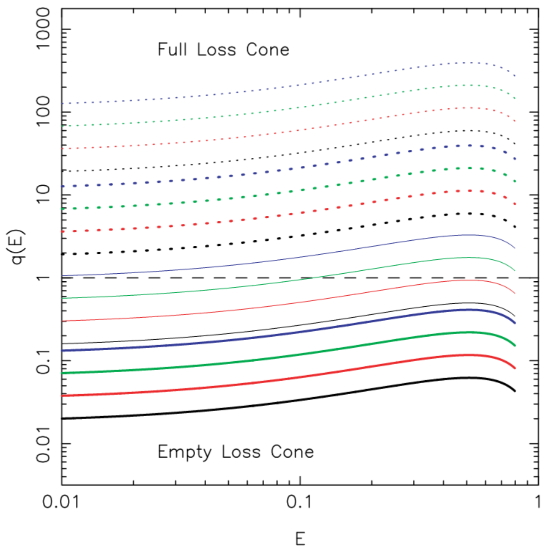

THE ASTROPHYSICAL JOURNAL, 633:680–687, 2005 November 10

LONG-TERM EVOLUTION OF MASSIVE BLACK HOLE BINARIES. II. BINARY EVOLUTION IN LOW-DENSITY GALAXIES

PETER BERCZIK,[1,2,3] DAVID MERRITT,[2] AND RAINER SPURZEM[3]

Slide from Li Shuo

Galaxy Collisions ≈ BH's collisions

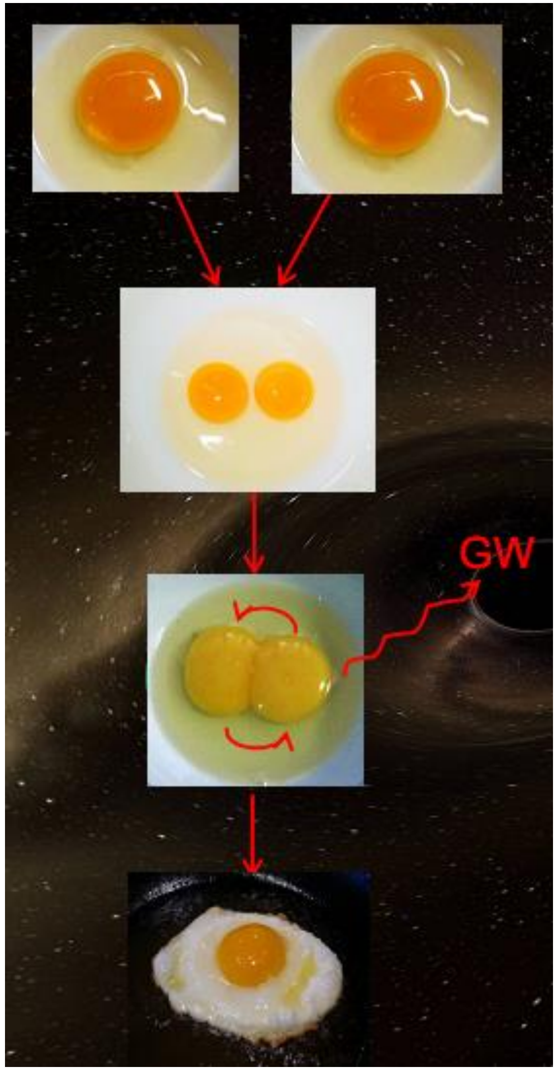

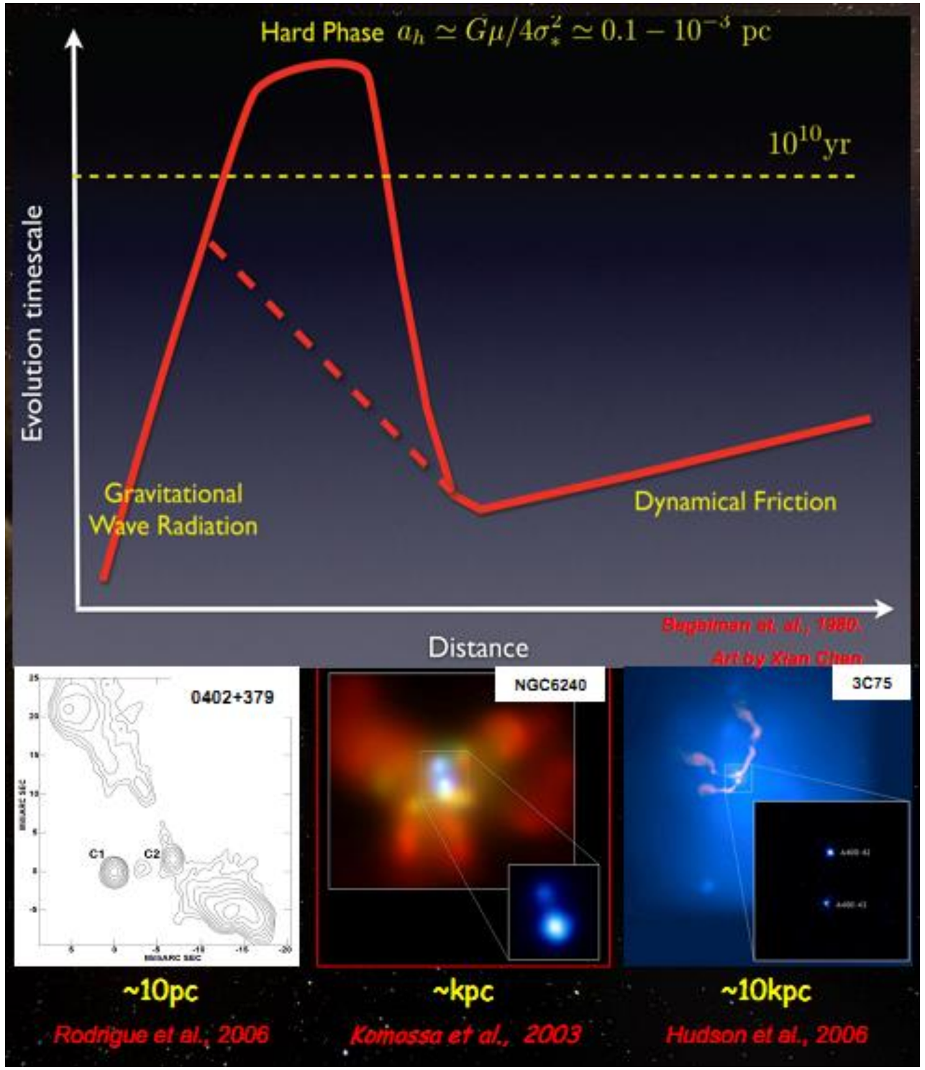

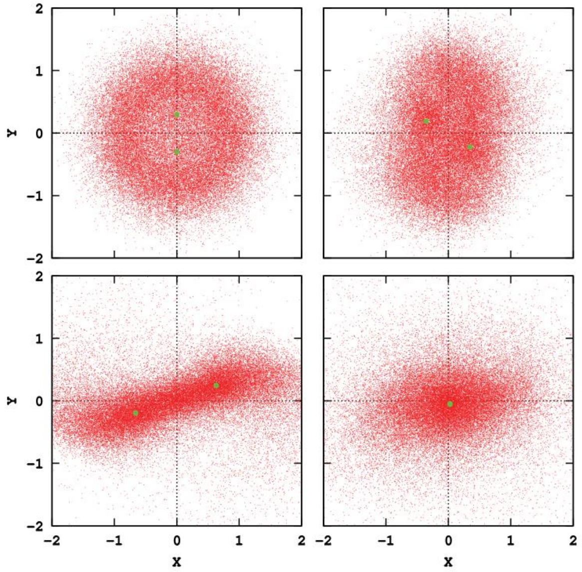

THE ASTROPHYSICAL JOURNAL, 642:L21–L24, 2006 May 1

EFFICIENT MERGER OF BINARY SUPERMASSIVE BLACK HOLES IN NONAXISYMMETRIC GALAXIES

PETER BERCZIK,[1,2,3] DAVID MERRITT,[1] RAINER SPURZEM,[2] AND HANS-PETER BISCHOF[4]

Slide from Li Shuo

MAO, Kiev 16 node GPU cluster

MAO 3+2 new nodes 4xGF 2080S + 4xGF 3070

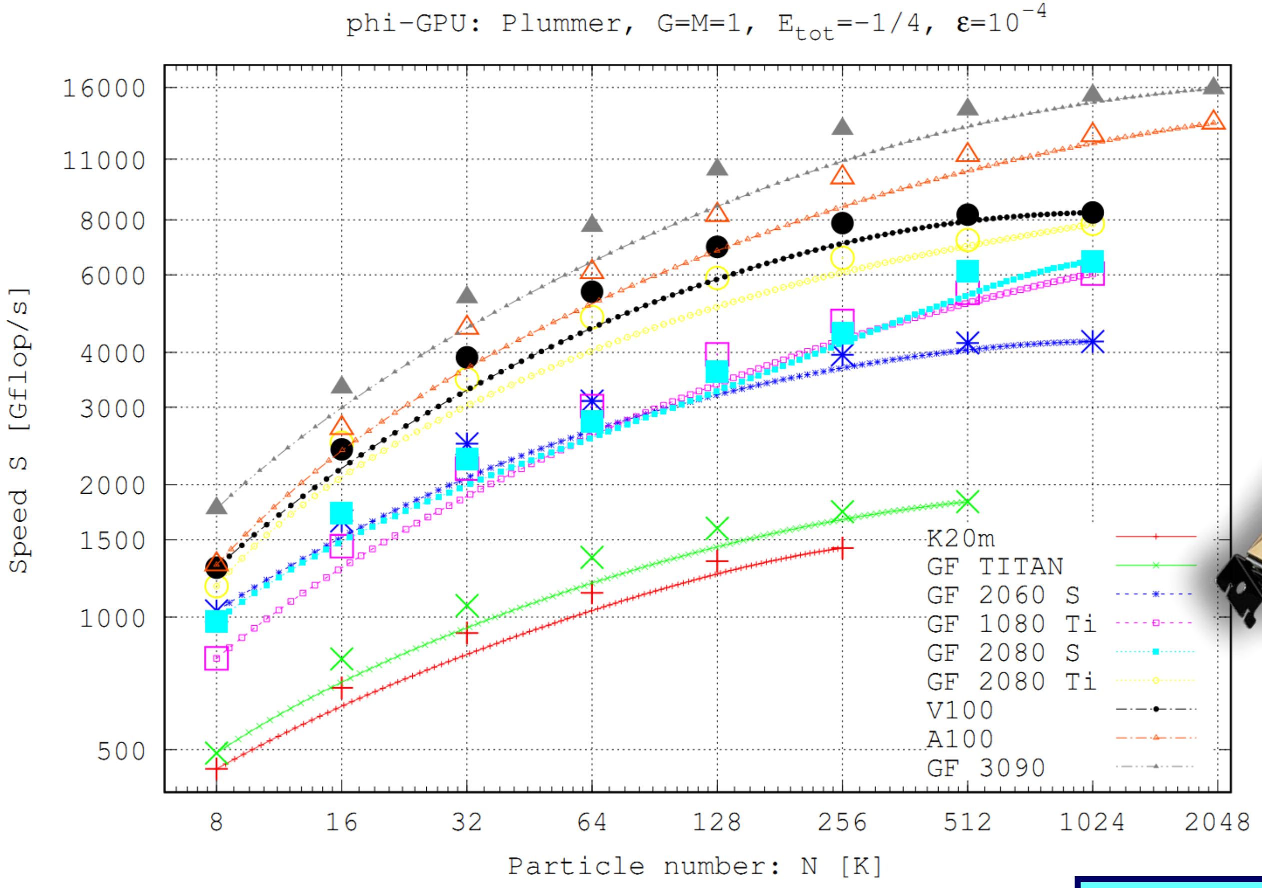

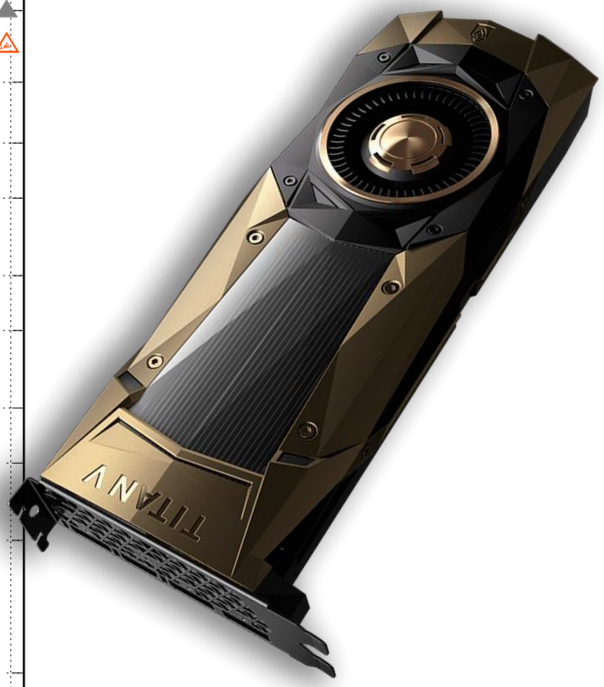

4 x GF 2080S, 3072 SP @ 1.81 GHz
4 x GF 3070, 5888 SP @ 1.77 GHz

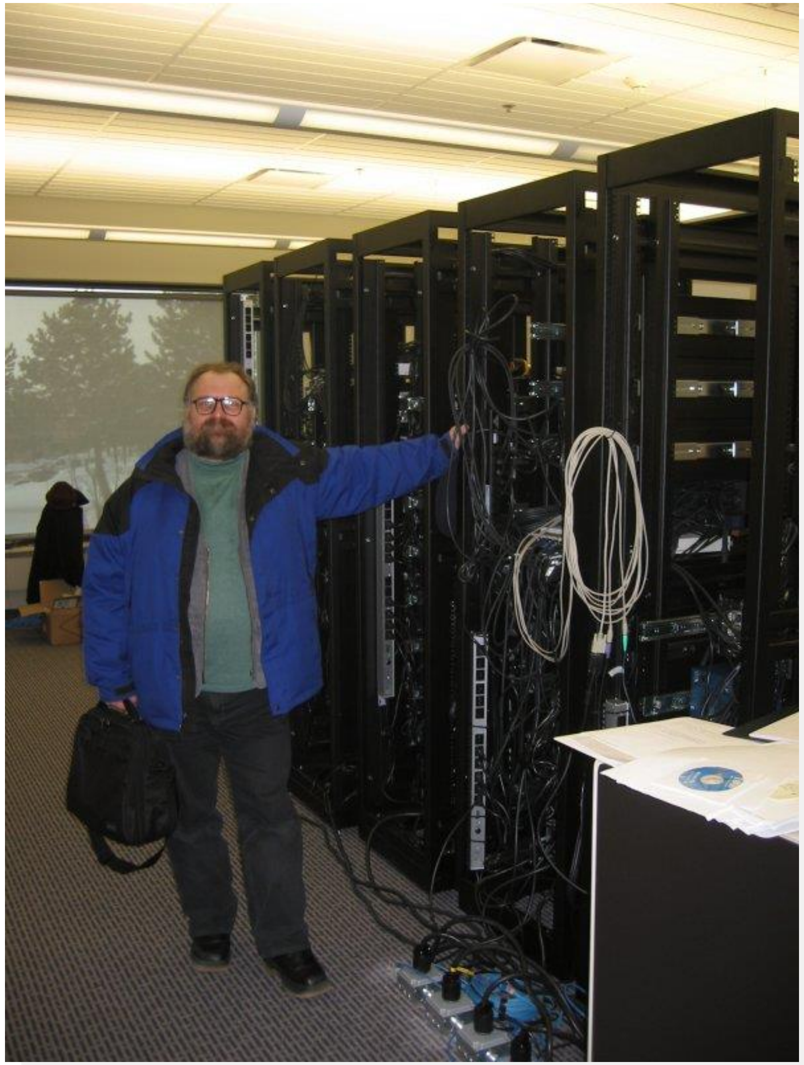


2005 11 21

JUWELS Booster consists of 936 compute nodes, each equipped with 4 NVIDIA A100 GPUs. The GPUs are hosted by AMD EPYC Rome CPUs. The compute nodes are connected with HDR-200 InfiniBand in a DragonFly+ topology.

The InfiniBand network of JUWELS Booster is implemented as a DragonFly+ network.

48 nodes are combined in a switch group (*cell*), interconnected in a full fat-tree topology, with 10 leaf switches and 10 spine switches in a two-level configuration. 40 Tbit/s of bi-section bandwidth is available.

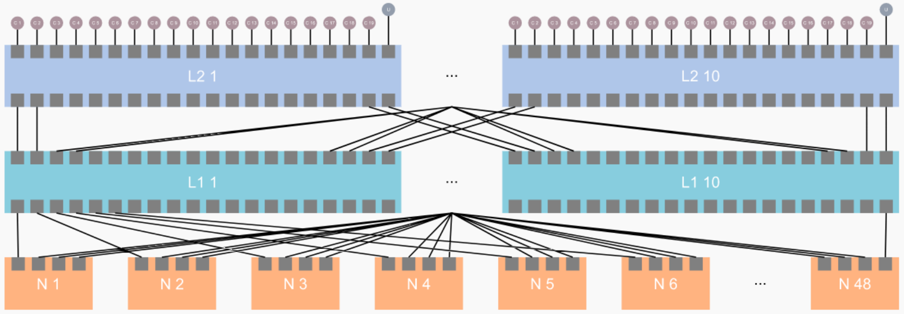

Sketch of the network topology within a JUWELS Booster cell with 48 nodes (`N1` to `N 48`), 10 level 1 switches (`L1 1` to `L1 10`) and 10 level 2 switches (`L2 1` to `L2 10`). Only a small subset of the total amount of links are shown for readability. The purple, 20th link leaving each level 2 switch should indicate the connection to JUWELS Cluster, while the other 19 outgoing level 2 links connect to other cells.

The configuration of JUWELS Booster compute nodes is the following

- **CPU**: AMD EPYC 7402 processor; 2 sockets, 24 cores per socket, SMT-2 (total: 2×24×2 = 96 threads) in NPS-4 [1] configuration (details on WikiChip)
- **Memory**: 512 GB DDR4-3200 RAM (of which at least 20 GB is taken by the system software stack, including the file system); 256 GB per socket; 8 memory channels per socket (2 channels per NUMA domain)
- **GPU**: 4 × NVIDIA A100 Tensor Core GPU with 40 GB; connected via NVLink3 to each other
- **Network**: 4 × Mellanox HDR200 InfiniBand ConnectX 6 (200 Gbit/s each), *HCA*
- **Periphery**: CPU, GPU, and network adapter are connected via 2 PCIe Gen 4 switches with 16 PCIe lanes going to each device (CPU socket: 2×16 lanes). PCIe switches are configured in *synthetic mode*.

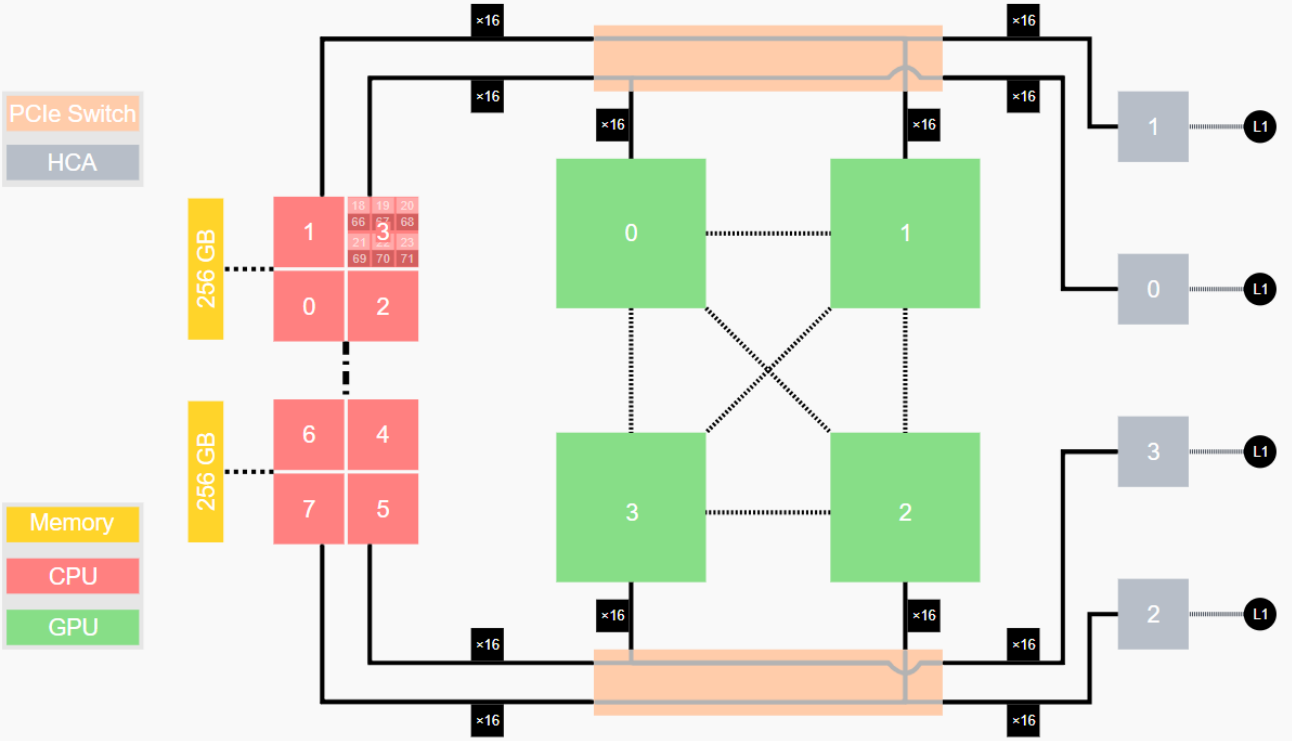

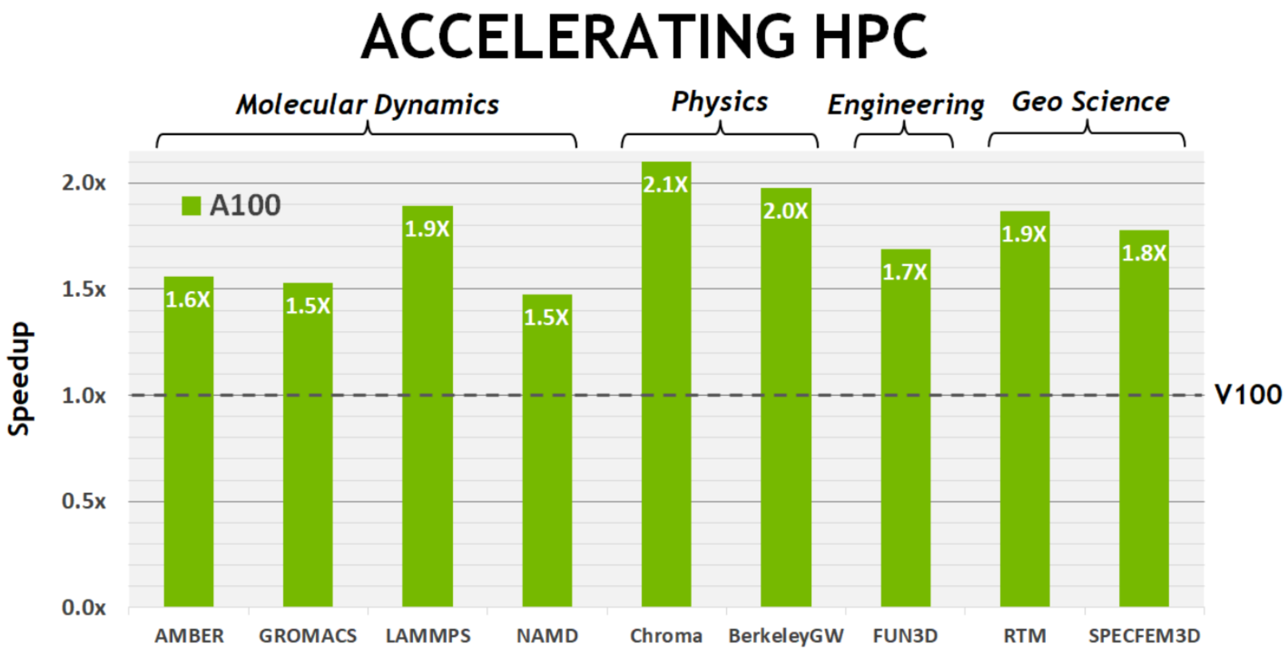

Peak FP64[1]	9.7 TFLOPS
Peak FP64 Tensor Core[1]	19.5 TFLOPS
Peak FP32[1]	19.5 TFLOPS
Peak FP16[1]	78 TFLOPS
Peak BF16[1]	39 TFLOPS
Peak TF32 Tensor Core[1]	156 TFLOPS | 312 TFLOPS[2]
Peak FP16 Tensor Core[1]	312 TFLOPS | 624 TFLOPS[2]
Peak BF16 Tensor Core[1]	312 TFLOPS | 624 TFLOPS[2]
Peak INT8 Tensor Core[1]	624 TOPS | 1,248 TOPS[2]
Peak INT4 Tensor Core[1]	1,248 TOPS | 2,496 TOPS[2]

Table 1. A100 Tensor Core GPU performance specs.
1) Peak rates are based on the GPU boost clock.
2) Effective TFLOPS / TOPS using the new Sparsity feature.

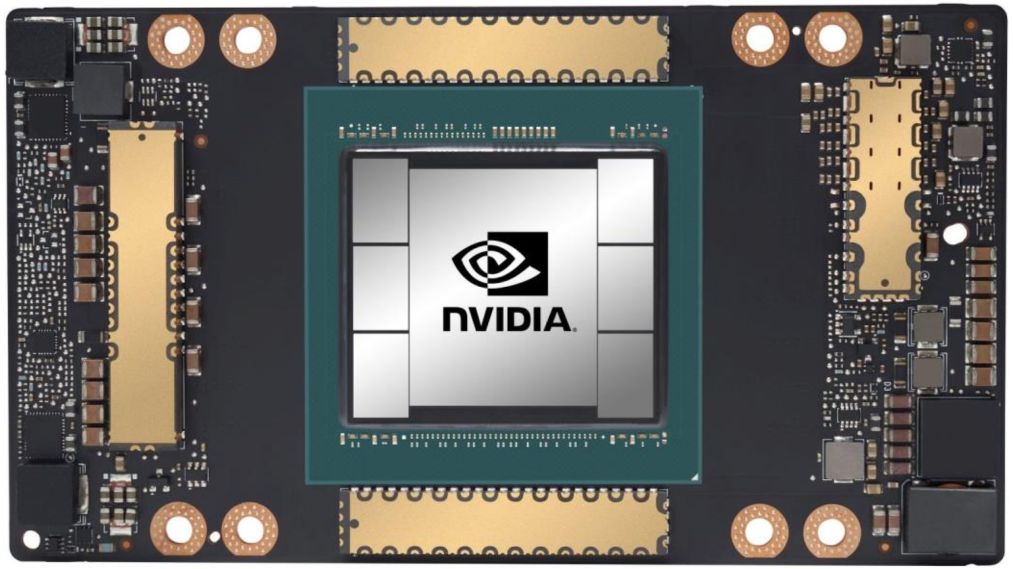

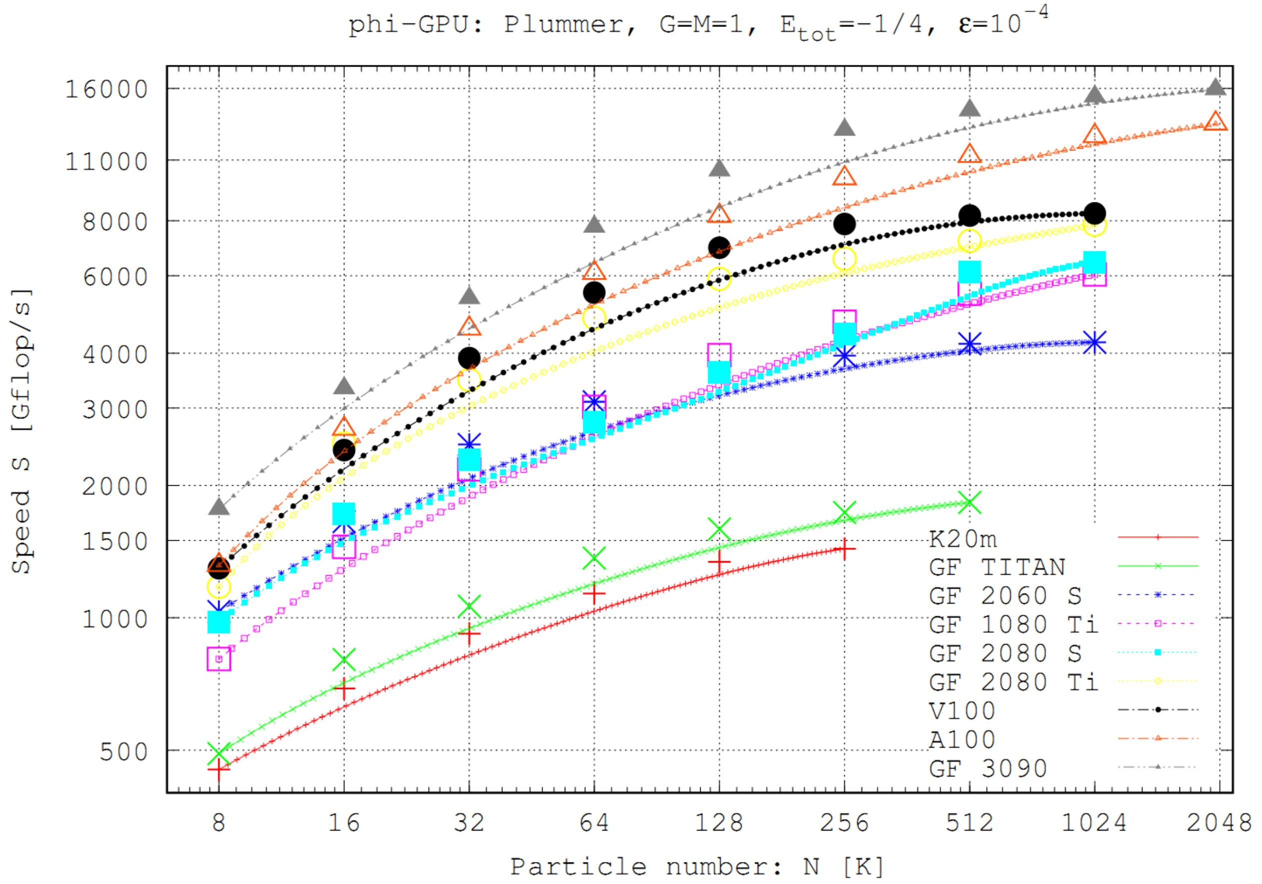

Our φGPU N-body code

Harfst et al, NewA, 12, 357 (2007)

Hierarchical Individual Block Time Steps

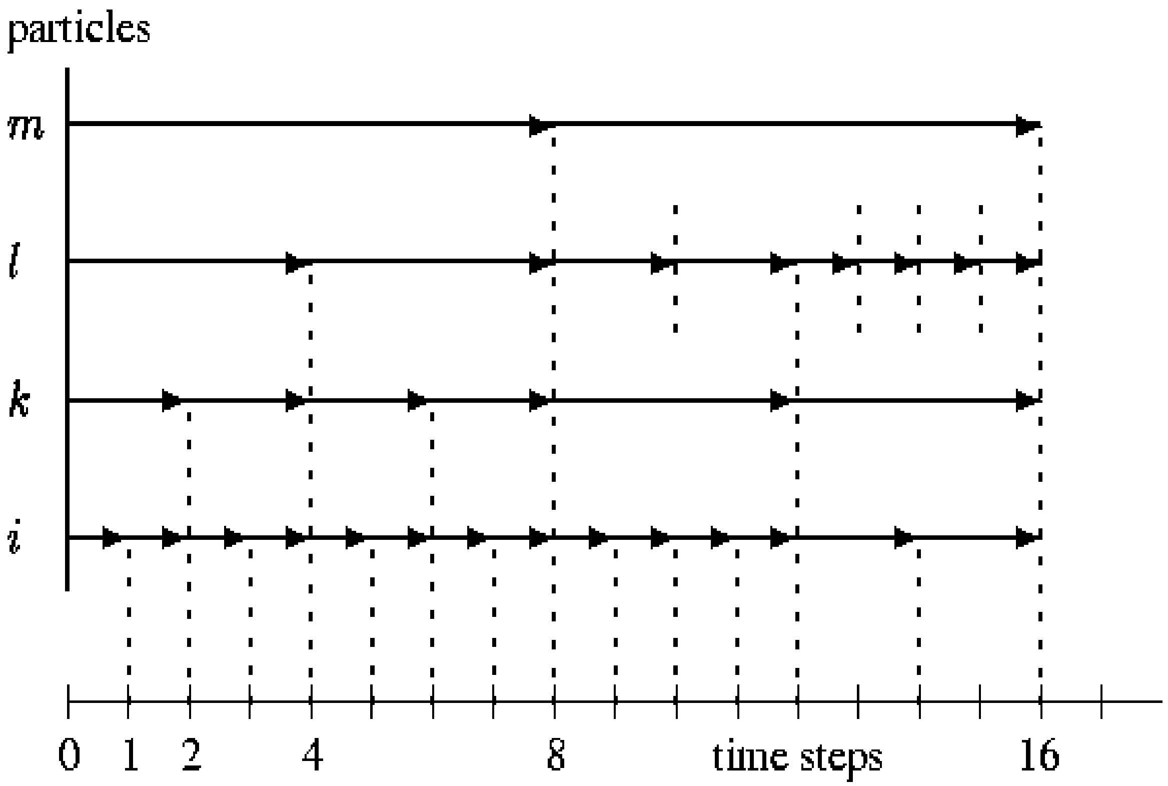

$$\Delta t = \sqrt{\eta \frac{|\vec{a}||\vec{a}^{(2)}| + |\dot{\vec{a}}|^2}{|\dot{\vec{a}}||\vec{a}^{(3)}| + |\vec{a}^{(2)}|^2}} \; .$$

4th order Hermite scheme

$$\frac{d^2 \vec{r}_i}{dt^2} = \vec{a}_i$$

https://github.com/berczik/phi-GPU-mole

Our φGPU N-body code

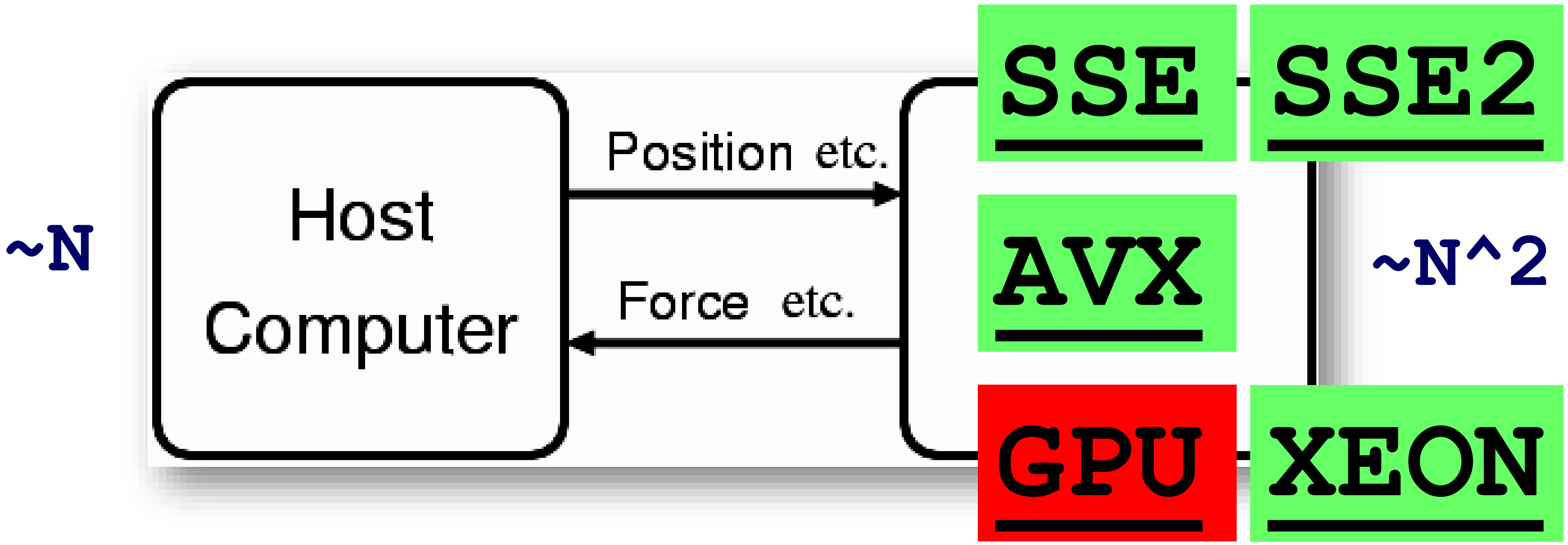

$$\vec{a}_i = \sum_{j=1;\, j \neq i}^{N} \vec{f}_{ij} \qquad \vec{f}_{ij} = -\frac{G \cdot m_j}{(r_{ij}^2 + \varepsilon^2)^{3/2}} \vec{r}_{ij}$$

https://github.com/berczik/phi-GPU-mole

Our φGPU "hybrid" N-body code

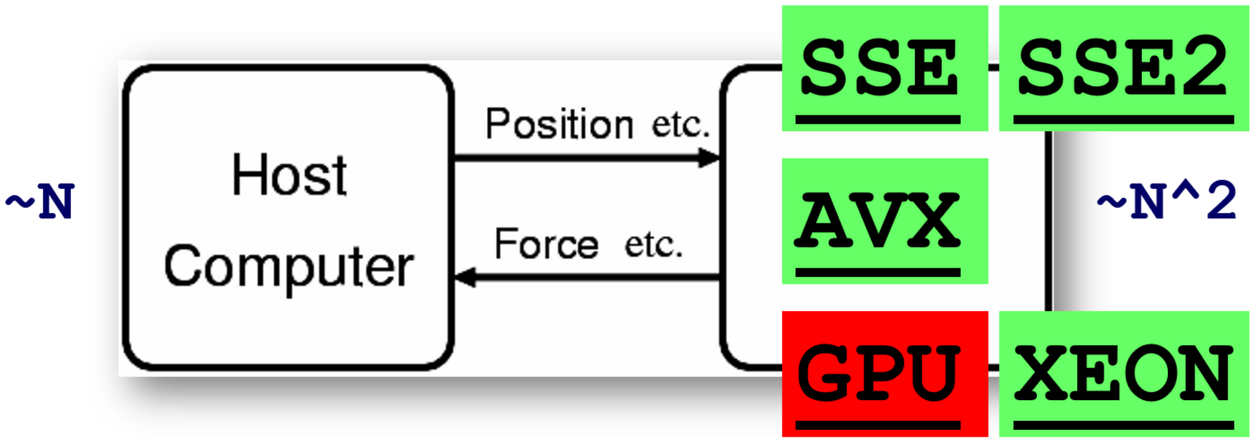

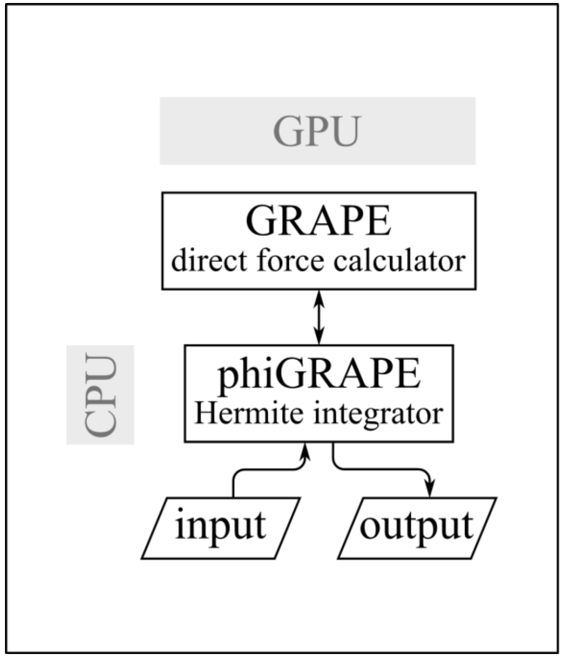

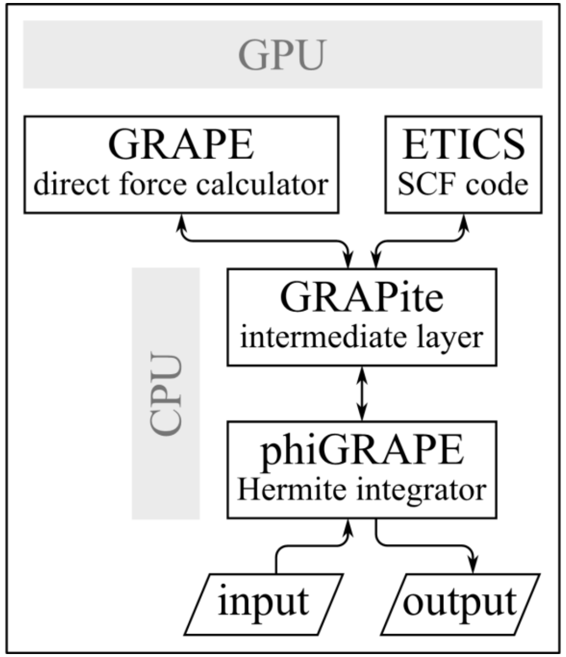

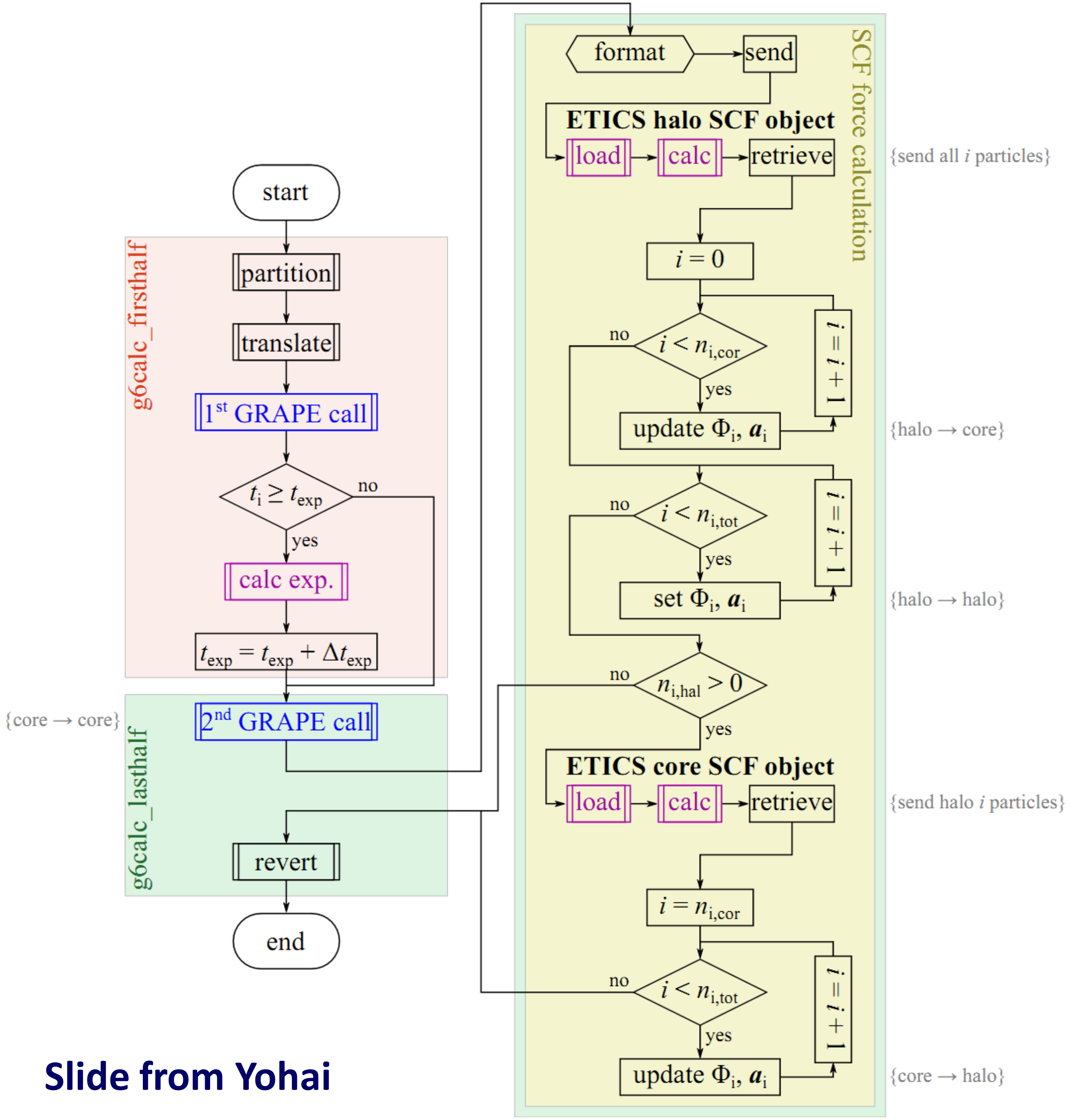

Slide from Yohai

Our φGPU N-body code

$$M(r) = M_o \cdot \frac{1}{(1+(r_o/r)^2)^{3/2}}$$

$$\rho(r) = \frac{3 \cdot M_o}{4\pi \cdot r_o{}^3} \cdot \frac{1}{(1+(r/r_o)^2)^{5/2}}$$

$$r_{HM} \approx 0.769$$

$$G = M = 1$$

$$E_{TOT} = -\frac{1}{4}$$

$$r_o = \frac{3\pi}{16} \approx 0.6$$

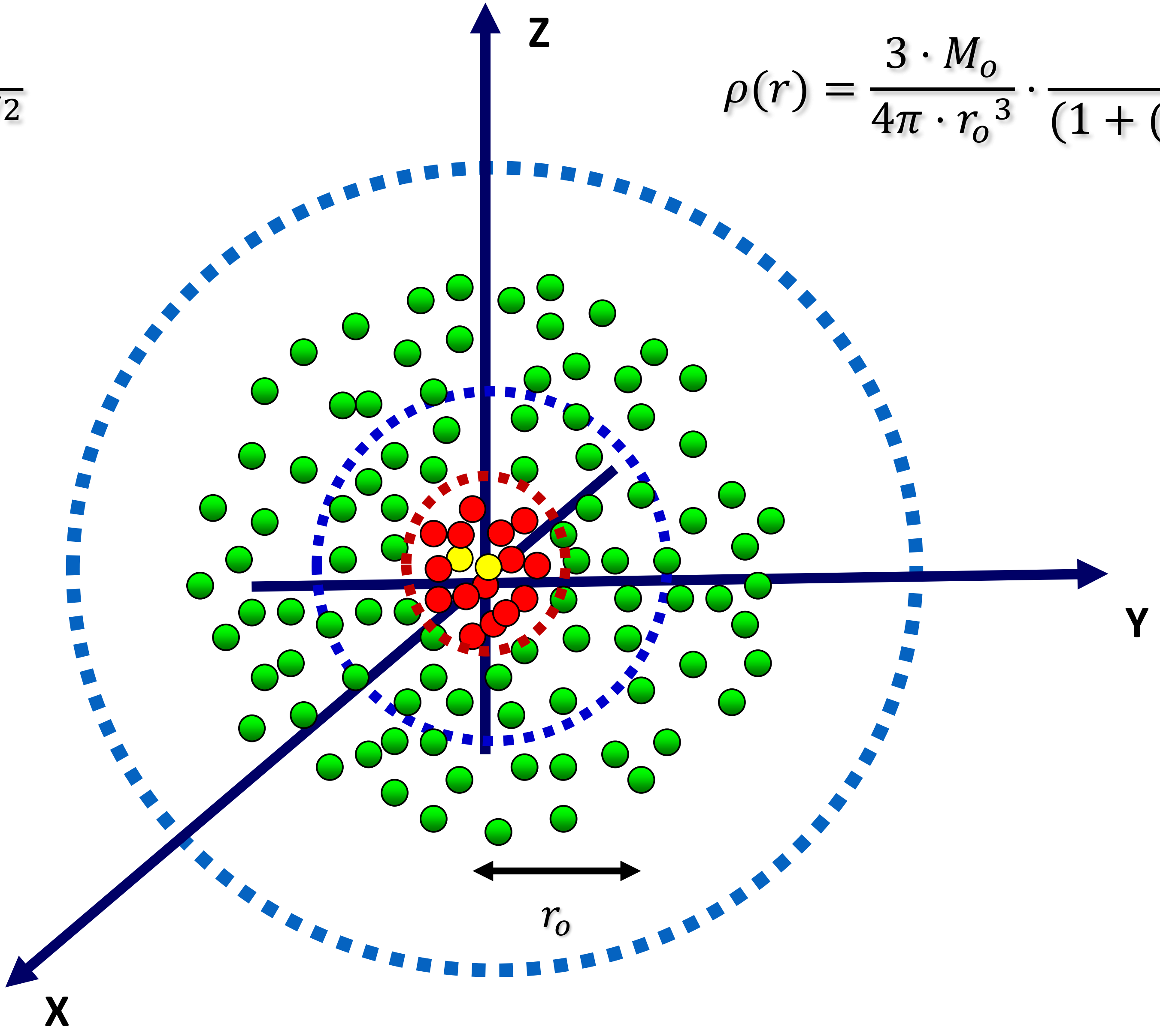

Initial Condition

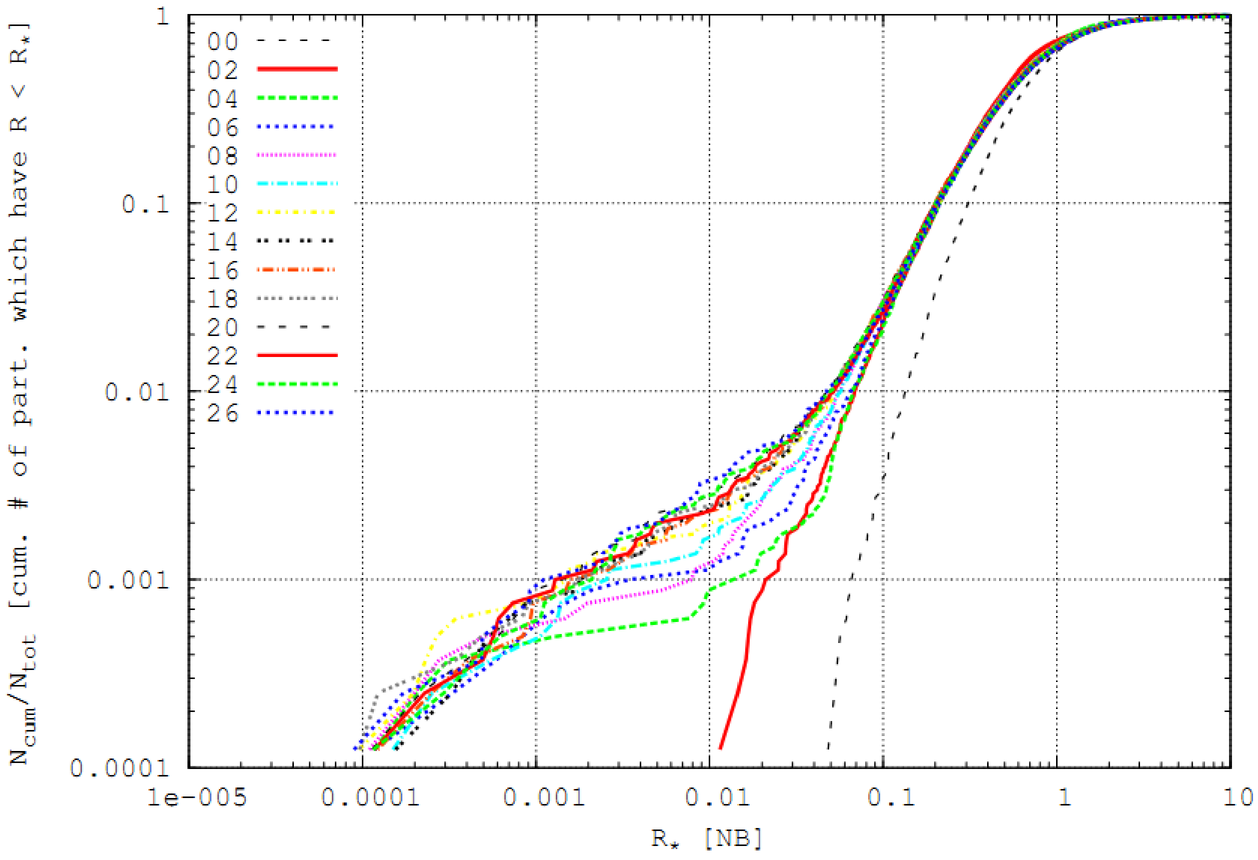

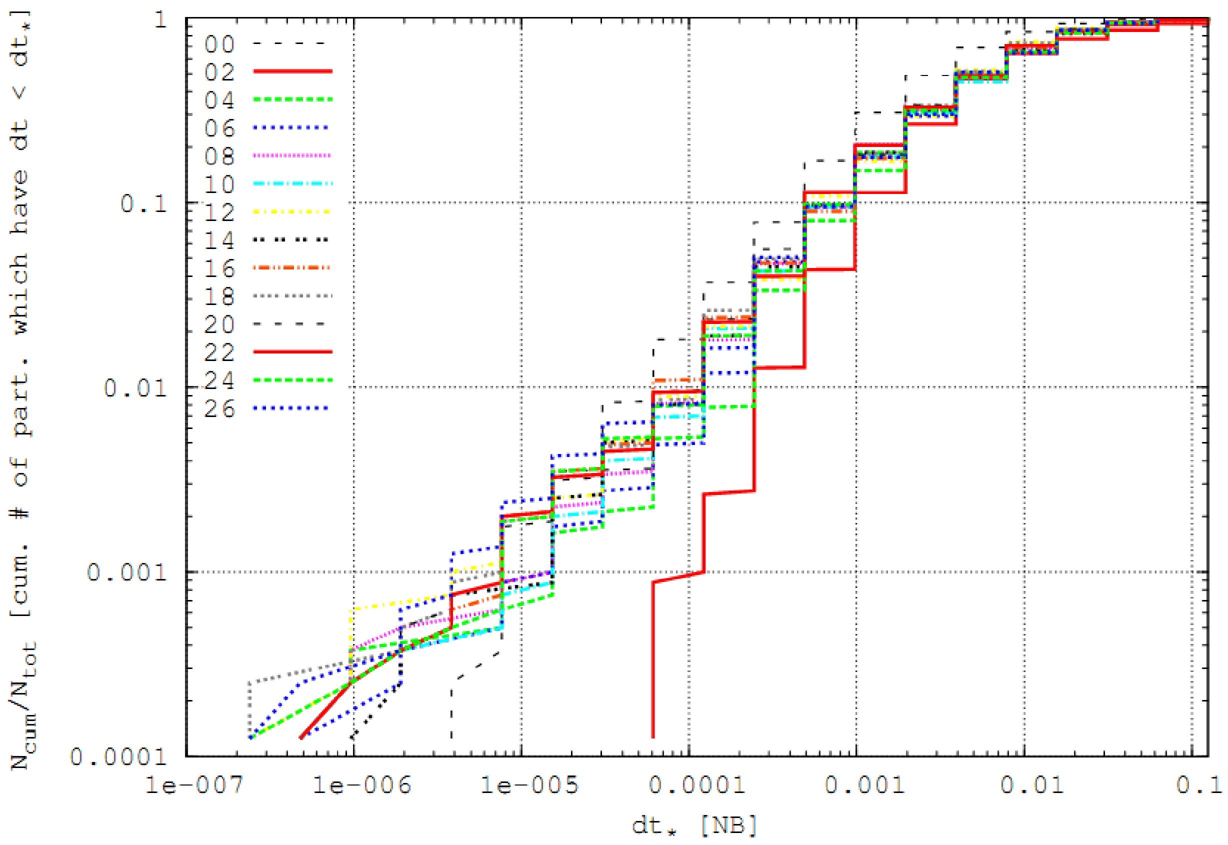

Our φGPU N-body code

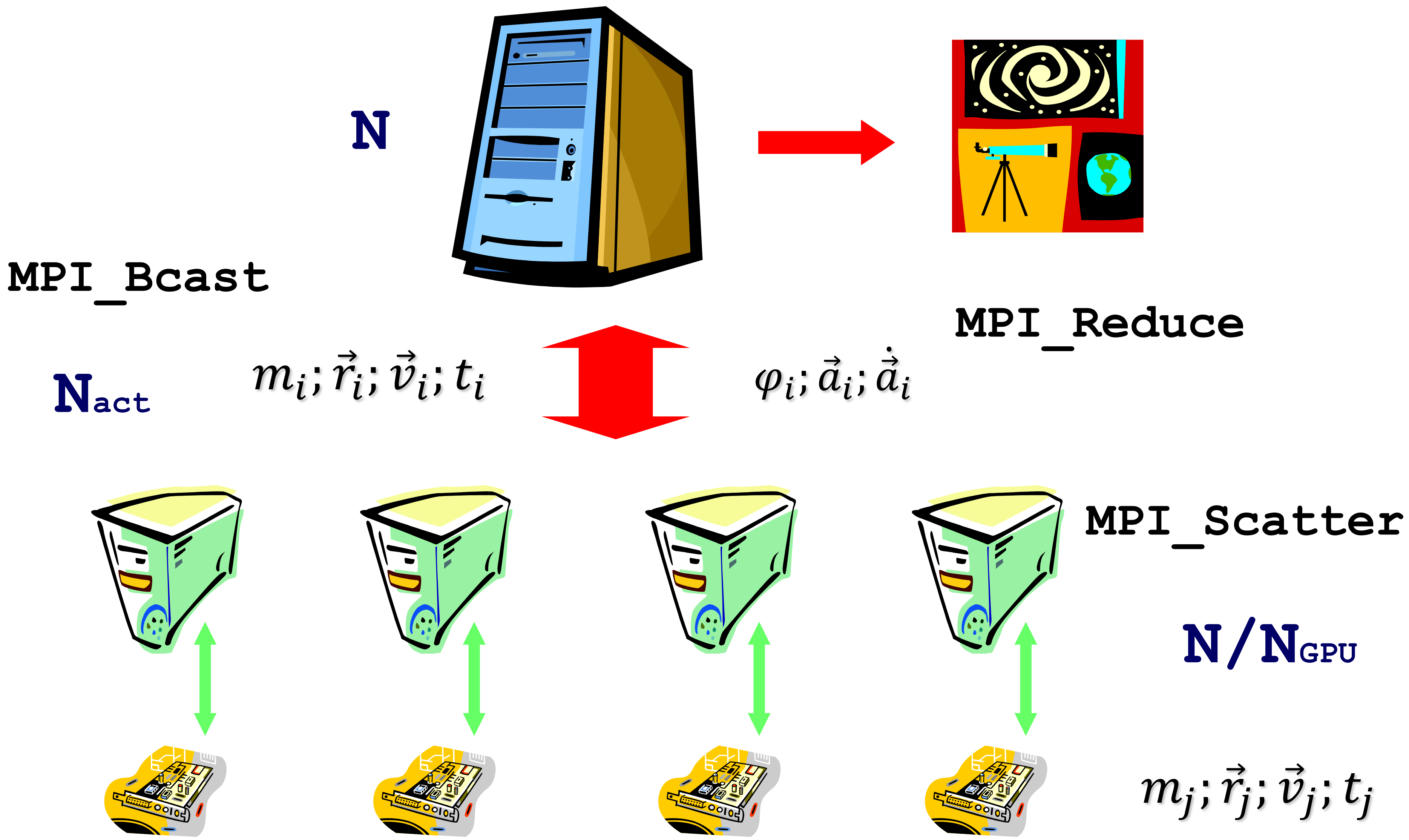

Our φGPU N-body code

$$i, j - particle$$

Some communication scheme…

$$N_{loc} = \frac{N}{N_{proc}}$$

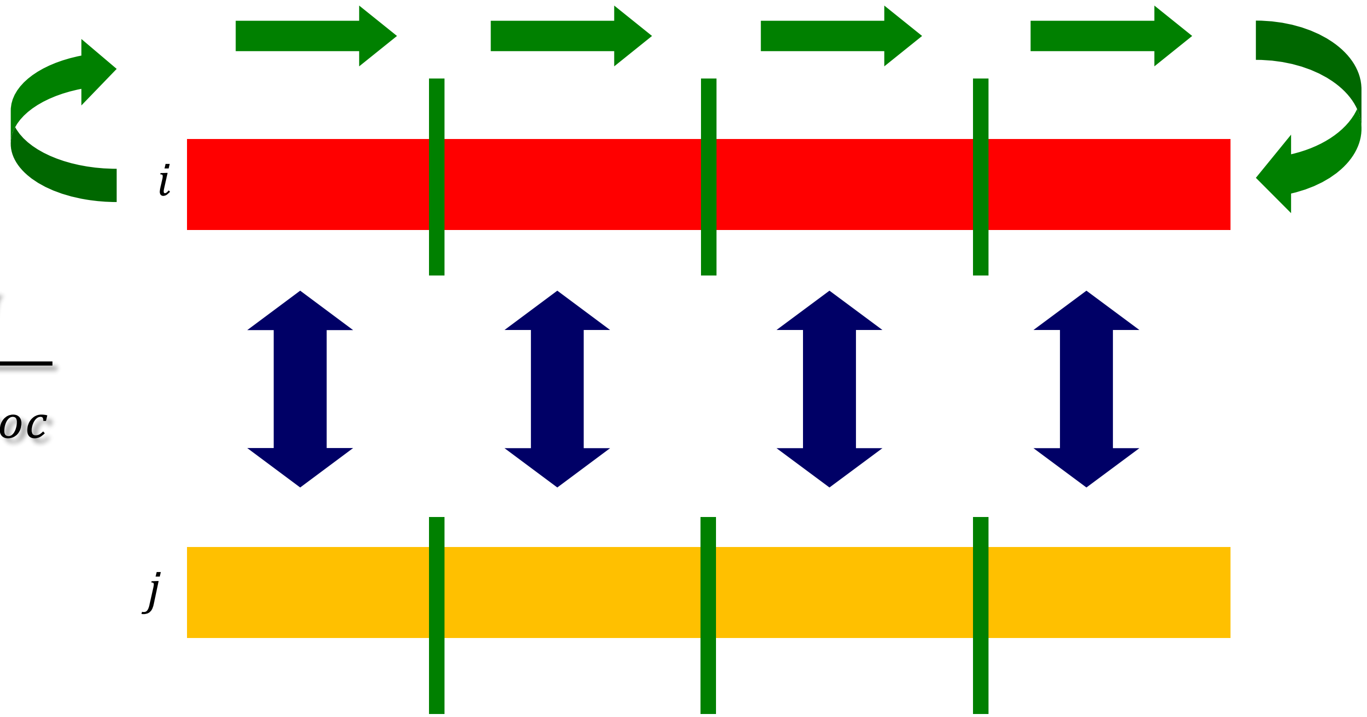

Our φGPU N-body code

$$\Delta T_{total} = \Delta T_{host} + \Delta T_{GPU} + \Delta T_{comm} + \Delta T_{MPI}$$

• active part. scan:	$O(N_{act} \log(N_{act}))$	$+T_{host}$
• all part. prediction:	$O(N/N_{GPU})$	$+T_{host}$
• ''j'' part. send. to GPU:	$O(N/N_{GPU})$	$+T_{comm}$
• ''i'' part. send. to GPU:	$O(N_{act})$	$+T_{comm}$
• ''force'' determ. on GPU:	$O(N\ N_{act}/N_{GPU})$	$+T_{GPU}$
• receive the ''force'':	$O(N_{act})$	$+T_{comm}$
• MPI global comm.:	$O((\tau_{lat}+N_{act}) \log(N_{GPU}))$	$+T_{MPI}$
• corr. for ''i'' part.:	$O(N_{act})$	$+T_{host}$

https://github.com/berczik/phi-GPU-mole

Our φGPU N-body code

$$\Delta T_{GPU} \propto N \cdot \frac{N_{act}}{N_{GPU}}$$

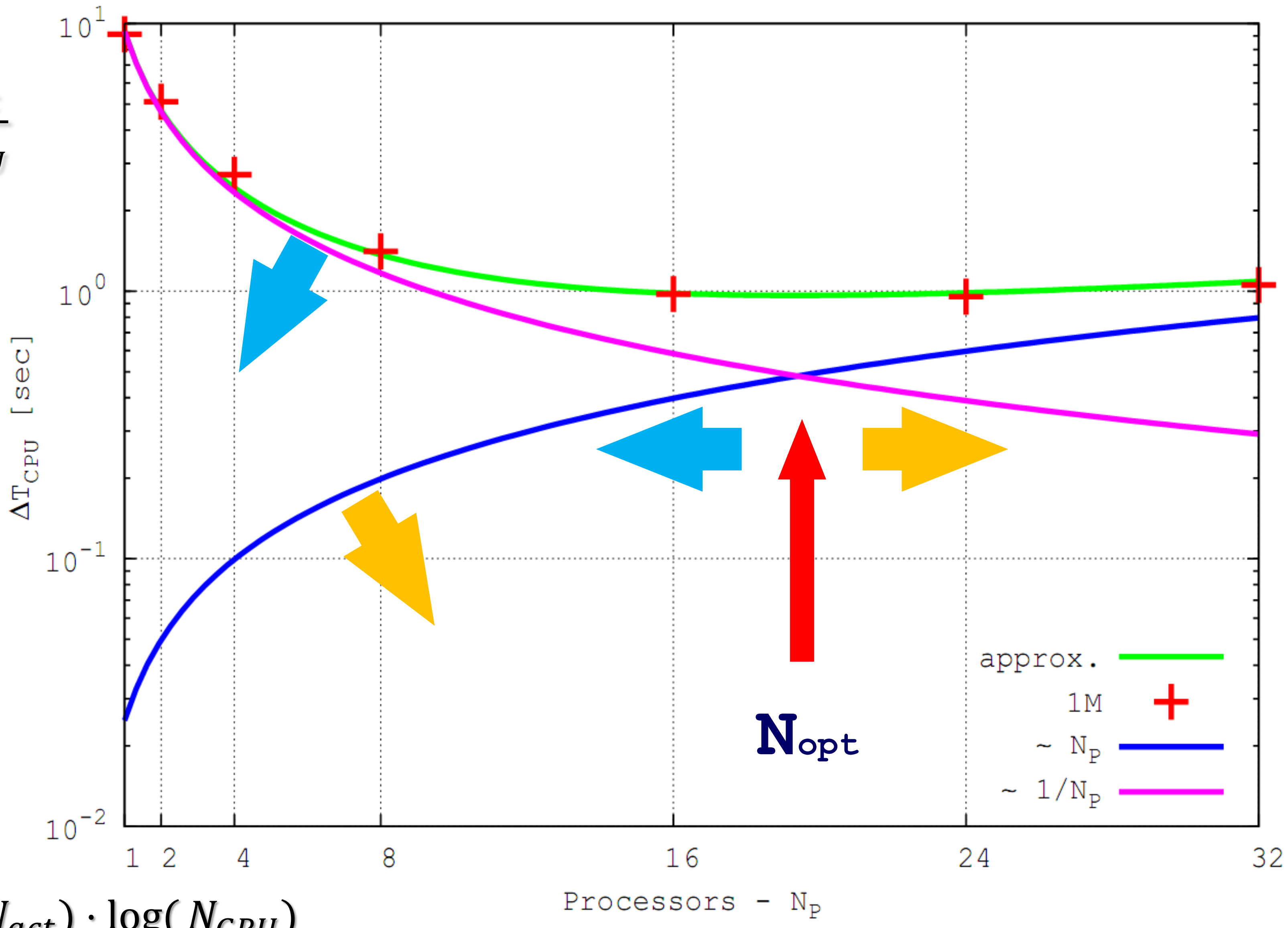

$$\Delta T_{MPI} \propto (\tau_{lat} + N_{act}) \cdot \log(N_{GPU})$$

Our φGPU N-body code

Tesla C2050 results **"mole-8.5" cluster**

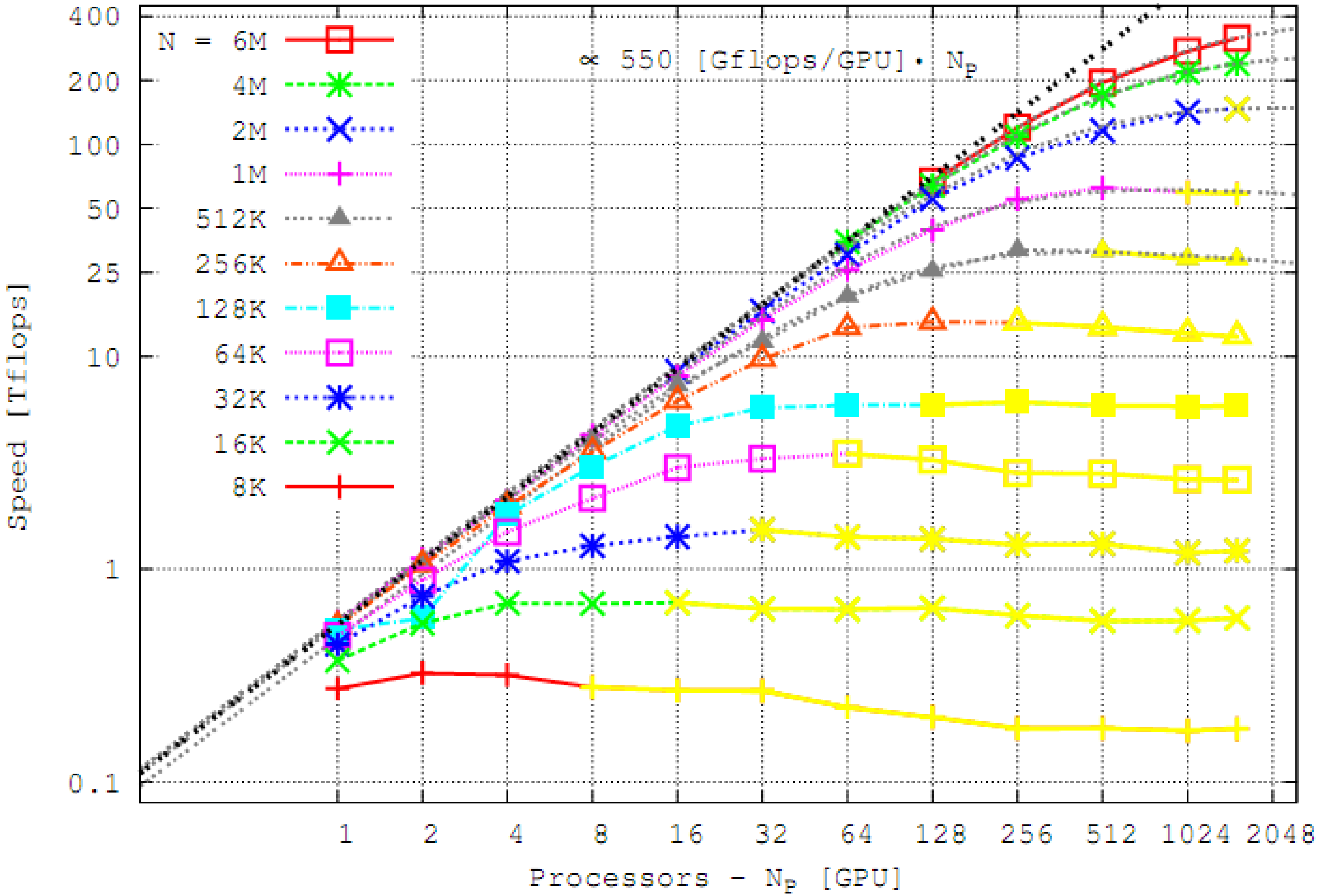

https://github.com/berczik/phi-GPU-mole

1536*448=688k cores

Our φGPU N-body code

Tesla C2050 results **"mole-8.5" cluster**

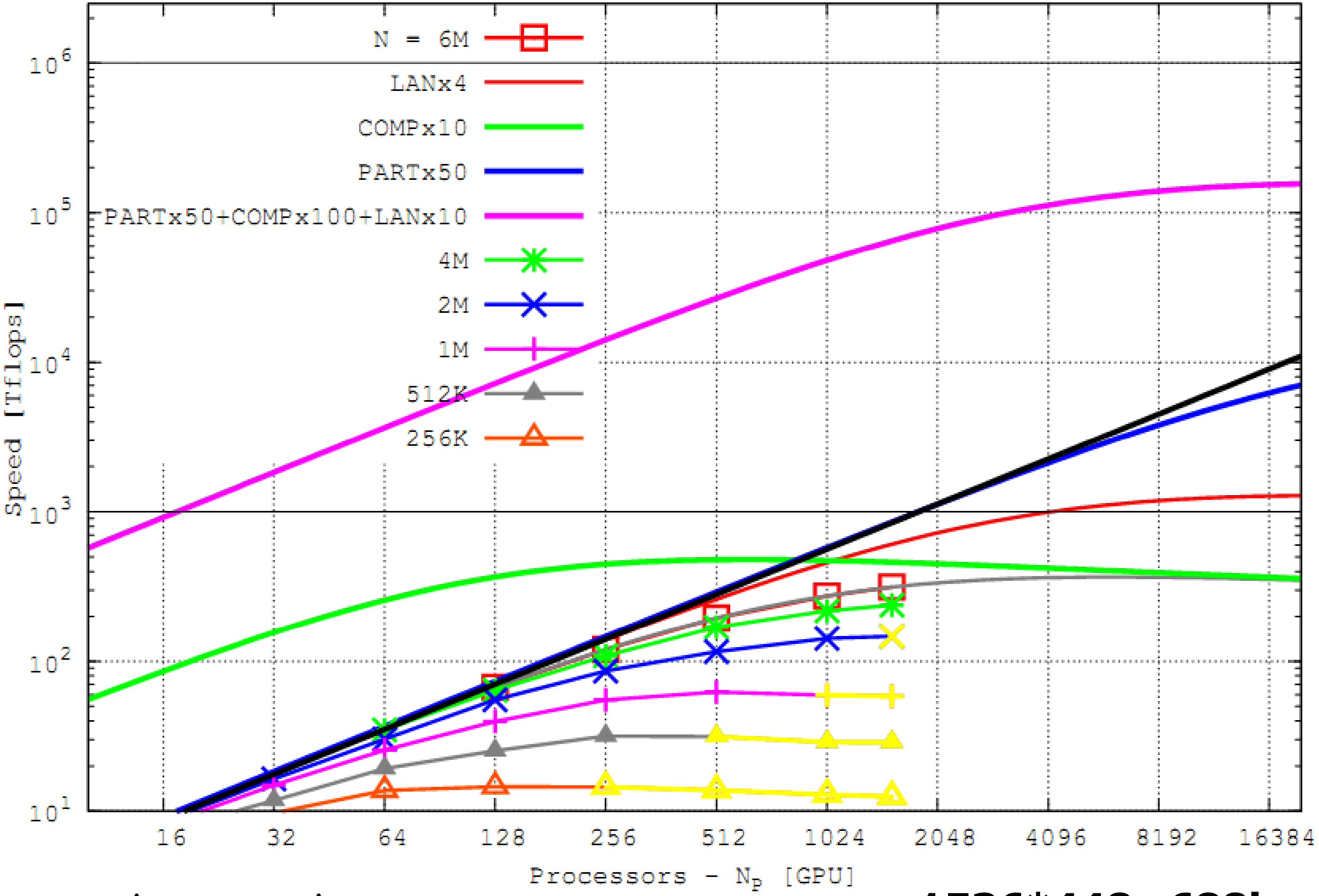

ExaFlops

PetaFlops

~64 A100 GPU

"A Man's Got To Know His Limitations"

Dirty Harry in Magnum Force (1973)

https://github.com/berczik/phi-GPU-mole

1536*448=688k cores

φGPU current usage/results

$$A^{(k)} = \left(|a^{(k-1)}||a^{(k+1)}| + |a^{(k)}|^2\right)^{1/2}$$

$$\Delta t = \eta \left(\frac{A^{(1)}}{A^{(p-2)}}\right)^{1/(p-3)}$$

mass distr.: Low mass + High mass.

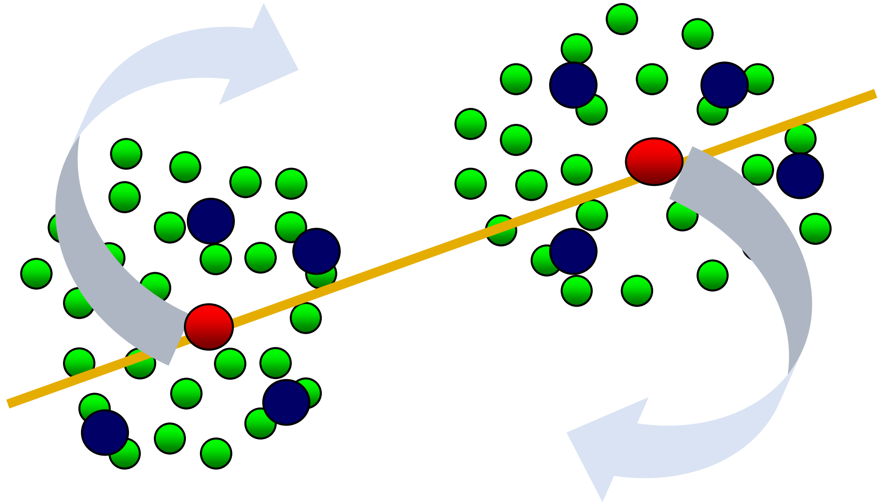

$$\epsilon_{ij}^2 = (\epsilon_i^2 + \epsilon_j^2)/2,$$

$$\frac{d\mathbf{v}}{dt} = -\frac{GM_\bullet}{r^2}\left[(1+\mathcal{A})\mathbf{n_{12}} + \mathcal{B}\mathbf{v_{12}}\right] + \mathcal{O}(1/c^8),$$

PN routine

$$\mathbf{a}_{\rm NoSpin} = \mathbf{a}_{\rm N} + \frac{1}{c^2}\mathbf{a}_{1\mathcal{PN}} + \frac{1}{c^4}\mathbf{a}_{2\mathcal{PN}} + \frac{1}{c^5}\mathbf{a}_{2.5\mathcal{PN}} + \frac{1}{c^6}\mathbf{a}_{3\mathcal{PN}} + \frac{1}{c^7}\mathbf{a}_{3.5\mathcal{PN}} + \mathcal{O}\left(\frac{1}{c^8}\right),$$

Blanchet 2006

Faye et al. 2006

Tagoshi et al. 2001

$$\mathbf{a}_{\rm Spin} = \mathbf{a}_{\rm NoSpin} + \frac{1}{c^3}\mathbf{a}_{1.5\mathcal{PN},\rm SO} + \frac{1}{c^4}\mathbf{a}_{2\mathcal{PN},\rm SS} + \frac{1}{c^5}\mathbf{a}_{2.5\mathcal{PN},\rm SO},$$

$$\frac{d\mathbf{v}}{dt} = -\frac{Gm}{r^2}[(1+A)\mathbf{n} + B\mathbf{v}].$$

Kupi et al. 2006; Berentzen et al. 2009; Brem 2013;
Sobolenko et al. 2016

$$\frac{d\vec{v}}{dt} = -\frac{Gm}{r^2}\left[(1+A)\vec{n} + B\vec{v}\right].$$

L. Blanchet. Gravitational Radiation from Post-Newtonian Sources and Inspiralling Compact Binaries. *Living Reviews in Relativity*, 9:4–+, June 2006.

$$\begin{aligned}
A =& \frac{1}{c^2}\left\{-\frac{3\dot{r}^2\eta}{2} + v^2 + 3\eta v^2 - \frac{Gm}{r}(4+2\eta)\right\} \\
&+ \frac{1}{c^4}\left\{\frac{15\dot{r}^4\eta}{8} - \frac{45\dot{r}^4\eta^2}{8} - \frac{9\dot{r}^2\eta v^2}{2} + 6\dot{r}^2\eta^2 v^2 + 3\eta v^4 - 4\eta^2 v^4\right. \\
&\quad \left. + \frac{Gm}{r}(-2\dot{r}^2 - 25\dot{r}^2\eta - 2\dot{r}^2\eta^2 - \frac{13\eta v^2}{2} + 2\eta^2 v^2) + \frac{G^2m^2}{r^2}(9 + \frac{87\eta}{4})\right\} \\
&+ \frac{1}{c^5}\left\{-\frac{24\dot{r}\eta v^2}{5}\frac{Gm}{r} - \frac{136\dot{r}\eta}{15}\frac{G^2m^2}{r^2}\right\} \\
&+ \frac{1}{c^6}\left\{-\frac{35\dot{r}^6\eta}{16} + \frac{175\dot{r}^6\eta^2}{16} - \frac{175\dot{r}^6\eta^3}{16} + \frac{15\dot{r}^4\eta v^2}{2} - \frac{135\dot{r}^4\eta^2 v^2}{4} + \frac{255\dot{r}^4\eta^3 v^2}{8}\right. \\
&\quad - \frac{15\dot{r}^2\eta v^4}{2} + \frac{237\dot{r}^2\eta^2 v^4}{8} - \frac{45\dot{r}^2\eta^3 v^4}{2} + \frac{11\eta v^6}{4} - \frac{49\eta^2 v^6}{4} + 13\eta^3 v^6 \\
&\quad + \frac{Gm}{r}(79\dot{r}^4\eta - \frac{69\dot{r}^4\eta^2}{2} - 30\dot{r}^4\eta^3 - 121\dot{r}^2\eta v^2 + 16\dot{r}^2\eta^2 v^2 + 20\dot{r}^2\eta^3 v^2 + \frac{75\eta v^4}{4} \\
&\quad + 8\eta^2 v^4 - 10\eta^3 v^4) \\
&\quad + \frac{G^2m^2}{r^2}(\dot{r}^2 + \frac{22717\dot{r}^2\eta}{168} + \frac{11\dot{r}^2\eta^2}{8} - 7\dot{r}^2\eta^3 + \frac{615\dot{r}^2\eta\pi^2}{64} - \frac{20827\eta v^2}{840} + \eta^3 v^2 \\
&\quad - \frac{123\eta\pi^2 v^2}{64}) \\
&\quad \left. + \frac{G^3m^3}{r^3}(-16 - \frac{1399\eta}{12} - \frac{71\eta^2}{2} + \frac{41\eta\pi^2}{16})\right\} \\
&+ \frac{1}{c^7}\left\{\frac{Gm}{r}(\frac{366}{35}\eta v^4 + 12\eta^2 v^4 - 114 v^2\eta\dot{r}^2 - 12\eta^2 v^2\dot{r}^2 + 112\eta\dot{r}^4)\right. \qquad (1.10) \\
&\quad + \frac{G^2m^2}{r^2}(\frac{692}{35}\eta v^2 - \frac{724}{15}v^2\eta^2 + \frac{294}{5}\eta\dot{r}^2 + \frac{376}{5}\eta^2\dot{r}^2) \\
&\quad \left. + \frac{G^3m^3}{r^3}(\frac{3956}{35}\eta + \frac{184}{5}\eta^2)\right\}
\end{aligned}$$

$$\begin{aligned}
B =& \frac{1}{c^2}\{-4\dot{r} + 2\dot{r}\eta\} \\
&+ \frac{1}{c^4}\left\{\frac{9\dot{r}^3\eta}{2} + 3\dot{r}^3\eta^2 - \frac{15\dot{r}\eta v^2}{2} - 2\dot{r}\eta^2 v^2 + \frac{Gm}{r}(2\dot{r} + \frac{41\dot{r}\eta}{2} + 4\dot{r}\eta^2)\right\} \\
&+ \frac{1}{c^5}\left\{\frac{8\eta v^2}{5}\frac{Gm}{r} + \frac{24\eta}{5}\frac{G^2m^2}{r^2}\right\} \\
&+ \frac{1}{c^6}\left\{-\frac{45\dot{r}^5\eta}{8} + 15\dot{r}^5\eta^2 + \frac{15\dot{r}^5\eta^3}{4} + 12\dot{r}^3\eta v^2 - \frac{111\dot{r}^3\eta^2 v^2}{4} - 12\dot{r}^3\eta^3 v^2 - \frac{65\dot{r}\eta v^4}{8}\right. \\
&\quad + 19\dot{r}\eta^2 v^4 + 6\dot{r}\eta^3 v^4 \\
&\quad + \frac{Gm}{r}(\frac{329\dot{r}^3\eta}{6} + \frac{59\dot{r}^3\eta^2}{2} + 18\dot{r}^3\eta^3 - 15\dot{r}\eta v^2 - 27\dot{r}\eta^2 v^2 - 10\dot{r}\eta^3 v^2) \\
&\quad \left. + \frac{G^2m^2}{r^2}(-4\dot{r} - \frac{5849\dot{r}\eta}{840} + 25\dot{r}\eta^2 + 8\dot{r}\eta^3 - \frac{123\dot{r}\eta\pi^2}{32})\right\} \\
&+ \frac{1}{c^7}\left\{\frac{Gm}{r}(-\frac{626}{35}\eta v^4 - \frac{12}{5}\eta^2 v^4 + \frac{678}{5}\eta v^2\dot{r}^2 + \frac{12}{5}\eta^2 v^2\dot{r}^2 - 120\eta\dot{r}^4)\right. \\
&\quad + \frac{G^2m^2}{r^2}(\frac{164}{21}\eta v^2 + \frac{148}{5}\eta^2 v^2 - \frac{82}{3}\eta\dot{r}^2 - \frac{848}{15}\eta^2\dot{r}^2) \\
&\quad \left. + \frac{G^3m^3}{r^3}(-\frac{1060}{21}\eta - \frac{104}{5}\eta^2)\right\}
\end{aligned}$$

4

$$\frac{d\vec{v}}{dt} = \vec{B}_{\text{NoSpin}} + \frac{1}{c^2}\vec{B}_{1.5PNSO} + \frac{1}{c^4}\vec{B}_{2PNSS} + \frac{1}{c^4}\vec{B}_{2.5PNSO}$$

$$h^{ij} = \frac{2G\mu}{Dc^4}\left[Q^{ij} + P^{0.5}Q^{ij} + PQ^{ij} + PQ^{ij}_{\rm SO} + P^{1.5}Q^{ij} + \ldots\right]_{\rm TT},$$

$$Q^{ij} = 2\left[v^i v^j - \frac{Gm}{r} n^i n^j\right]$$

$$h^{ij} \approx \frac{4G\mu}{Dc^4}\left[v^i v^j - \frac{Gm}{r} n^i n^j\right]$$

$$\begin{aligned} \epsilon^{ij}_{+} &= \hat{e}^i_y \hat{e}^j_y - \hat{e}^i_x \hat{e}^j_x \\ \epsilon^{ij}_{\times} &= \hat{e}^i_x \hat{e}^j_y + \hat{e}^i_y \hat{e}^j_x, \end{aligned}$$

$$\begin{aligned} \hat{e}_x &= (1,0,0) \\ \hat{e}_y &= (0,1,0) \\ \hat{e}_z &= (0,0,1), \end{aligned}$$

$$\epsilon^{ij}_{+} = \begin{pmatrix} 0 & 0 & 0 \\ 0 & 1 & 0 \\ 0 & 0 & -1 \end{pmatrix}$$

$$\epsilon^{ij}_{\times} = \begin{pmatrix} 0 & 0 & 0 \\ 0 & 0 & 1 \\ 0 & 1 & 0 \end{pmatrix}$$

$$\begin{aligned} h_{+} &= h^{ij}\epsilon^{+}_{ij} \\ h_{\times} &= h^{ij}\epsilon^{\times}_{ij}. \end{aligned}$$

SWIFT COALESCENCE OF SUPERMASSIVE BLACK HOLES IN COSMOLOGICAL MERGERS OF MASSIVE GALAXIES

The Astrophysical Journal, 828:73 (8pp), 2016 September 10

Mahmood Khan[1], Davide Fiacconi[2], Lucio Mayer[2], Peter Berczik[3,4,5], and Andreas Just[4]

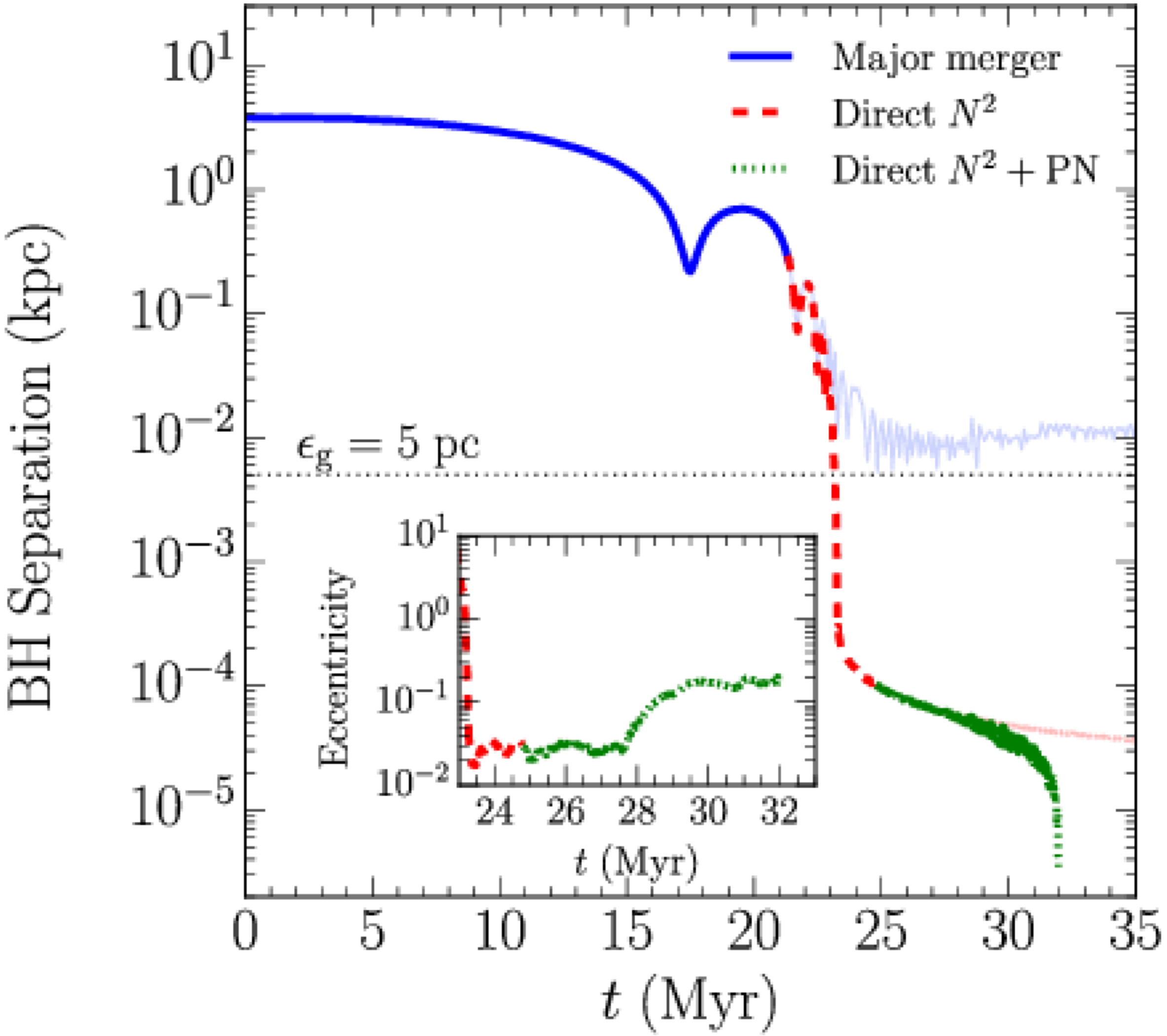

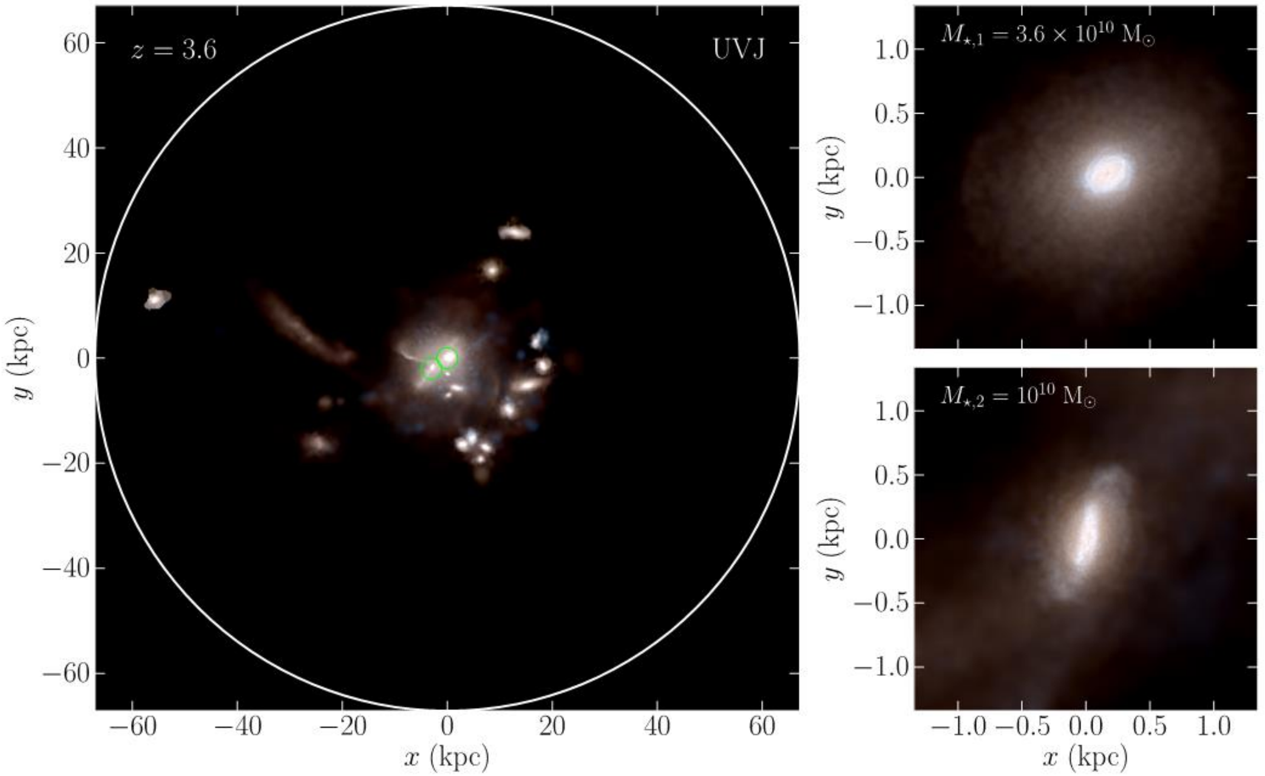

THE ASTROPHYSICAL JOURNAL, 868:97 (11pp), 2018 December 1

Dynamical Evolution and Merger Timescales of LISA Massive Black Hole Binaries in Disk Galaxy Mergers

Fazeel M. Khan[1], Pedro R. Capelo[2], Lucio Mayer[2], and Peter Berczik[3,4,5]

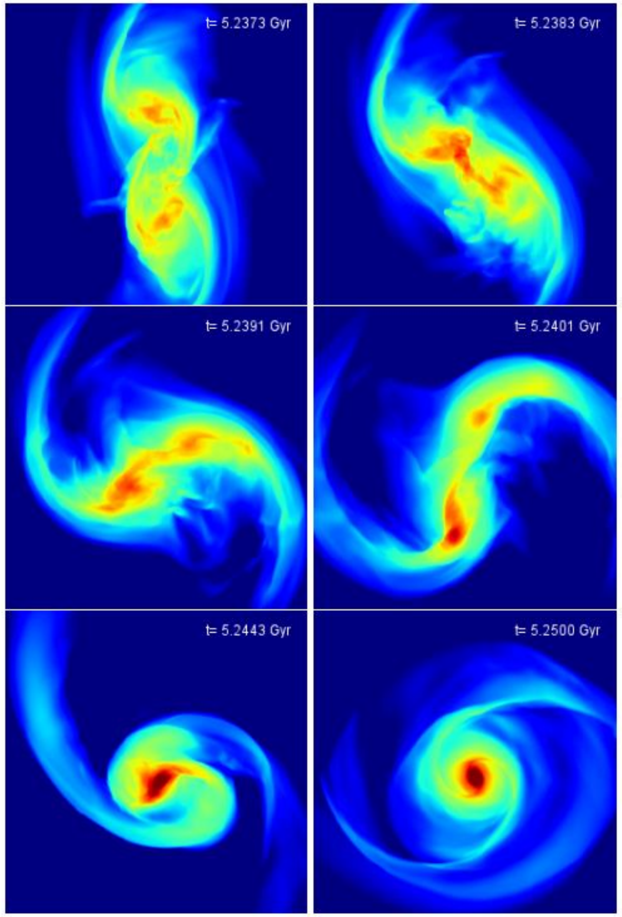

Figure 1. Mass-weighted gas density maps during last pericenter and final merger. The line-of-sight is perpendicular to the orbital plane and the maps are 1.8 kpc wide. While fairly symmetric before the pericenter (top left), the density distribution becomes clearly asymmetric after the pericenter (middle). After the final merger, a thick $\sim 10^9$ $M_\odot$ gaseous nuclear disk is formed (bottom), in which the two SMBHs start orbiting.

1:10 – 1:3 minor merger

Two SMBH's ~10^6 Mₒ

High accuracy direct summation: ~3 – 6 M Particles!

First time reach the < 1 mpc separation of BBH from initial ~1 kpc scale

Full up to 3.5 PN accurate BBH dynamics!

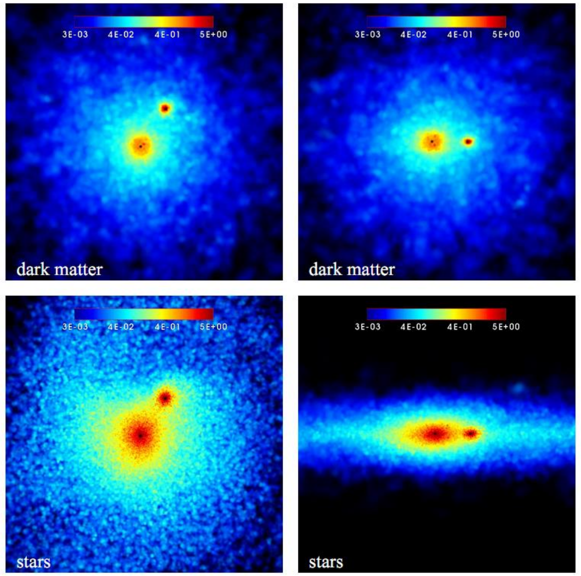

FIG. 1.— Density distribution of the dark matter (top panels) and stellar component (bottom panels) in the $x-y$ (left column) and $y-z$ (right column) planes. The two high density regions are clearly visible around the two SMBHs (black dots) in the center. The size of each box is 4 kpc.

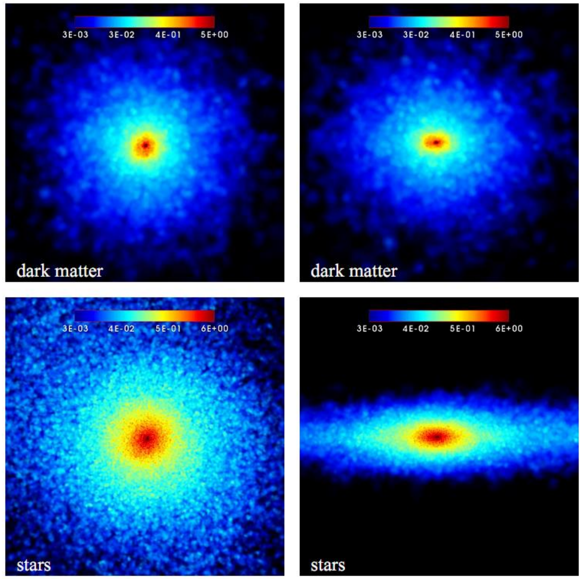

FIG. 3.— Same as in Figure 1 but at $T = 40$ Myr. Both SMBHs are embedded in a single cusp.

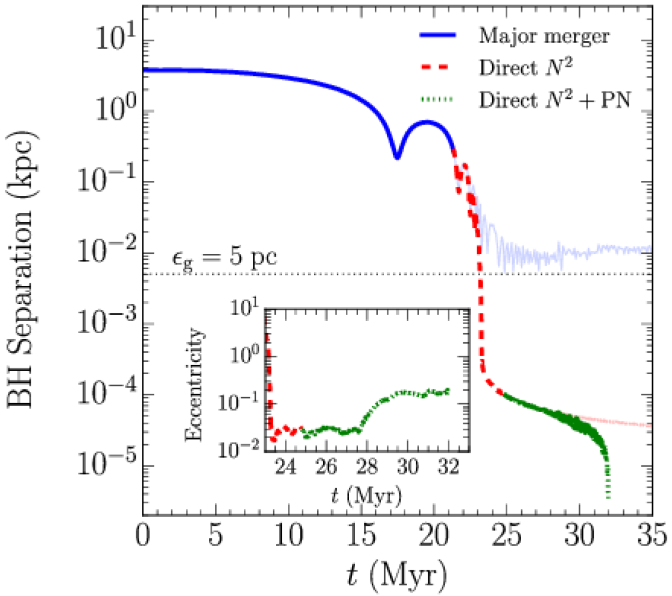

A&A 615, A71 (2018)
https://doi.org/10.1051/0004-6361/201730489

Gravitational wave driven mergers and coalescence time of supermassive black holes

Fazeel Mahmood Khan[1], Peter Berczik[2,3], and Andreas Just[4]

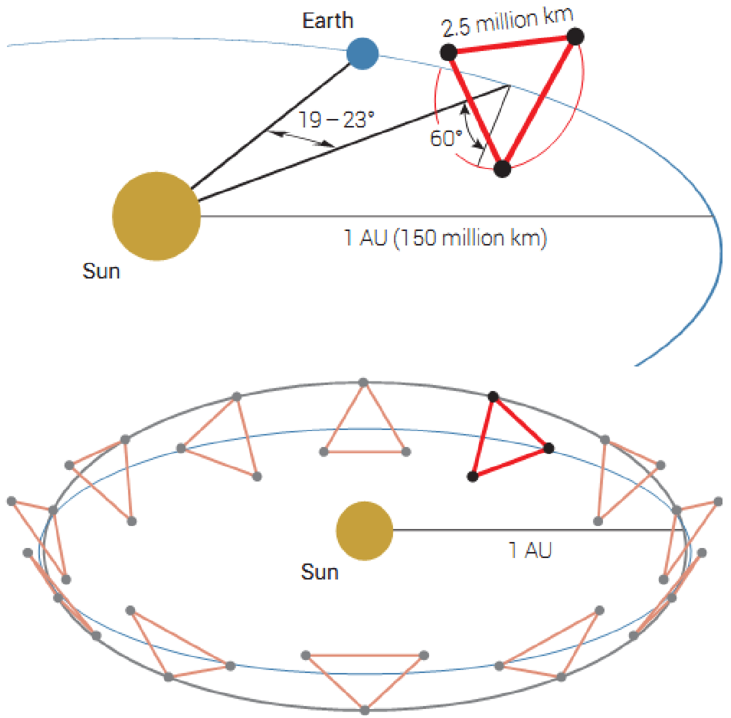

Figure 4: Depiction of the LISA Orbit.

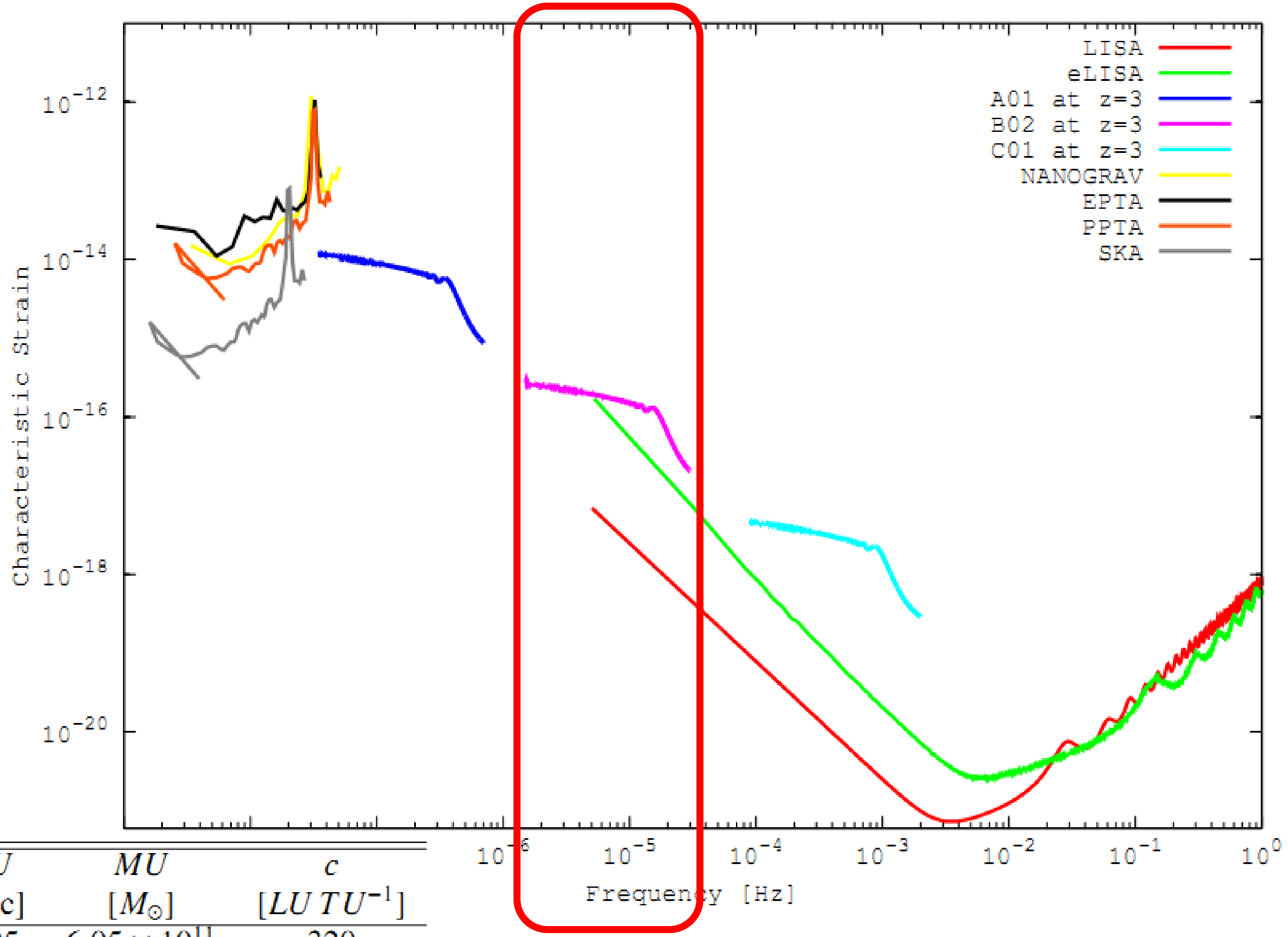

Series	Galaxy	$M_\bullet$ [$M_\odot$]	$\sigma_\star$ [km s^{-1}]	r_h [pc]	TU [Myr]	LU [kpc]	MU [$M_\odot$]	c [$LU\,TU^{-1}$]
A	M87	6.05×10^9	325	255	3.07	2.95	6.05×10^{11}	320
B	M31	1.63×10^8	169	21.75	1.01	0.42	1.63×10^{10}	733
C	MW	4.6×10^6	103	1.4	0.62	.092	4.6×10^8	2044

A&A 665, A86 (2022)
https://doi.org/10.1051/0004-6361/202244354

Astronomy & Astrophysics

Merging of unequal mass binary black holes in non-axisymmetric galactic nuclei

Peter Berczik[1,2,3], Manuel Arca Sedda[4], Margaryta Sobolenko[3], Marina Ishchenko[3], Olexander Sobodar[3], and Rainer Spurzem[1,5]

Table 1. Set of parameters of our model runs.

m_1 10^{-2} (1)	m_2 10^{-2} (2)	M_{12} 10^{-2} (3)	q (4)	μ 10^{-2} (5)	025k (6)	050k (7)	100k (8)	200k (9)	400k (10)	1M (11)
1	0.01	1.01	0.010	0.0099	–	–	450	–	–	–
1	0.02	1.02	0.020	0.0196	–	–	450	–	–	–
1	0.03	1.03	0.030	0.0291	–	–	350	–	–	–
1	0.05	1.05	0.050	0.0476	–	–	350	–	–	–
1	0.10	1.10	0.100	0.0909	250	250	250$^{(*)}$	250	250	150
1	0.20	1.20	0.200	0.1666	250	250	250$^{(*)}$	250	250	150
1	0.50	1.50	0.500	0.3333	250	250	250$^{(*)}$	250	250	150
1	1.00	2.00	1.000	0.5000	250	250	250$^{(*)}$	250	250	150
2	0.02	2.02	0.010	0.0198	–	–	450	–	–	–
2	0.03	2.03	0.015	0.0295	–	–	450	–	–	–
2	0.05	2.05	0.025	0.0488	–	–	350	–	–	–
2	0.10	2.10	0.050	0.0952	–	–	350	–	–	–
2	0.20	2.20	0.100	0.1818	–	–	250	–	–	–
2	0.40	2.40	0.200	0.3333	–	–	250	–	–	–
2	1.00	3.00	0.500	0.6666	250	250	250	250	250	150
2	2.00	4.00	1.000	1.0000	250	250	250	250	250	150
4	0.04	4.04	0.010	0.0396	–	–	450	–	–	–
4	0.08	4.08	0.020	0.0784	–	–	450	–	–	–
4	0.10	4.10	0.025	0.0976	–	–	350	–	–	–
4	0.20	4.20	0.050	0.1905	–	–	350	–	–	–
4	0.40	4.40	0.100	0.3636	–	–	250	–	–	–
4	0.80	4.80	0.200	0.6666	–	–	250	–	–	–
4	2.00	6.00	0.500	1.3333	250	250	250	250	250	150
4	4.00	8.00	1.000	2.0000	250	250	250	250	250	150

Notes. Final integration time in N-body units. Columns 1 and 2: SMBH masses (primary and secondary, respectively) in a 10^{-2} model units. Column 3: total mass $M_{12} = m_1 + m_2$ in 10^{-2} model units. Column 4: mass ratio $q = m_2/m_1$, where $m_2 \geq m_1$. Column 5: reduced mass $\mu \equiv m_1 m_2/(m_1 + m_2)$ in 10^{-2} model units. Columns 6–11: Particle number in the stellar galactic nucleus. $^{(*)}$ In these simulations, we performed two independent sets of runs. After the first set of runs, where the initial orbital velocity of the SMBH was exactly circular, $V_{\rm circ}$, we ran a second set of runs where the initial velocity of the SMBHs was $V_{\rm red} = 0.1\, V_{\rm circ}$.

$$\frac{da}{dt} = \left.\frac{da}{dt}\right|_{*} + \left.\frac{da}{dt}\right|_{\rm GW},$$
$$\frac{de}{dt} = \left.\frac{de}{dt}\right|_{*} + \left.\frac{de}{dt}\right|_{\rm GW},$$

$$\left.\frac{da}{dt}\right|_{\rm GW} = -\frac{64\beta}{5}\frac{F(e)}{a^3},$$
$$\beta = \frac{G^3}{c^5 m_1 m_2 (m_1 + m_2)},$$
$$F(e) = (1-e^2)^{-7/2}\left(1 + \frac{73}{24}e^2 + \frac{37}{96}e^4\right).$$

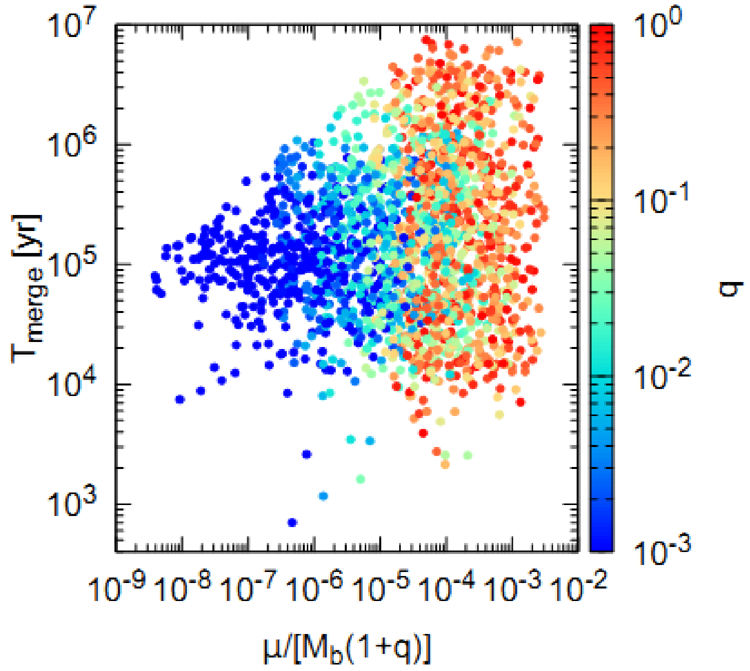

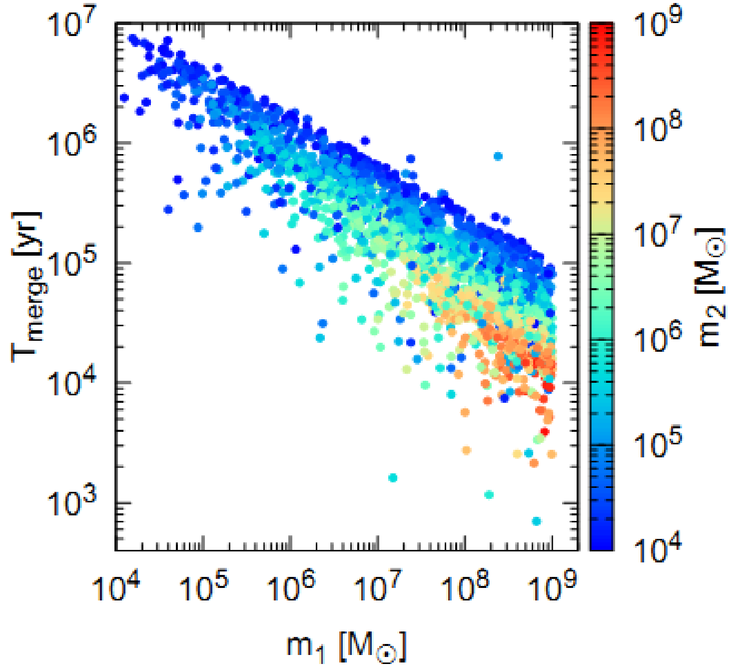

A&A 658, A152 (2022)
https://doi.org/10.1051/0004-6361/202140827

Astronomy & Astrophysics

First direct dynamical detection of a dual supermassive black hole system at sub-kiloparsec separation

Karina T. Voggel[1], Anil C. Seth[2], Holger Baumgardt[3], Bernd Husemann[4], Nadine Neumayer[4], Michael Hilker[5], Renuka Pechetti[6], Steffen Mieske[7], Antoine Dumont[2], and Iskren Georgiev[4]

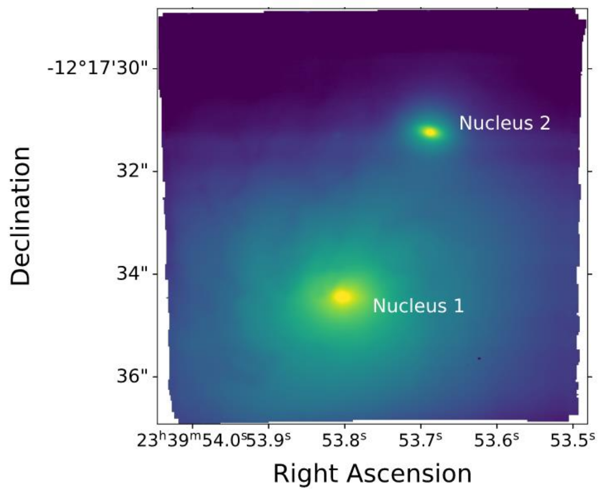

Fig. 1. White-light image of the collapsed MUSE data cube. Nucleus 1 is the photometric center of the main galaxy NGC 7727, and Nucleus 2 is offset to the north-west, which is 500 pc in projected separation.

Table 3. Summary of the main results for Nuclei 1 and 2.

Name	Nucleus 1	Nucleus 2
RA	23:39:53.796	23:39:53.679
Dec	−12:17:34.04	−12:17:30.83
$M_{\rm BH}$ [$M_\odot$]	$1.54^{+0.18}_{-0.15} \times 10^8$	$6.33^{+3.32}_{-1.40} \times 10^6$
$M_{\rm Bulge}$ [$M_\odot$]	5.24×10^{10}	2.10×10^8
Integrated σ [km s^{-1}]	191.2 ± 1.5	66.3 ± 1.3
Velocity [km s^{-1}]	1794.9 ± 1.9	1839.2 ± 1.8

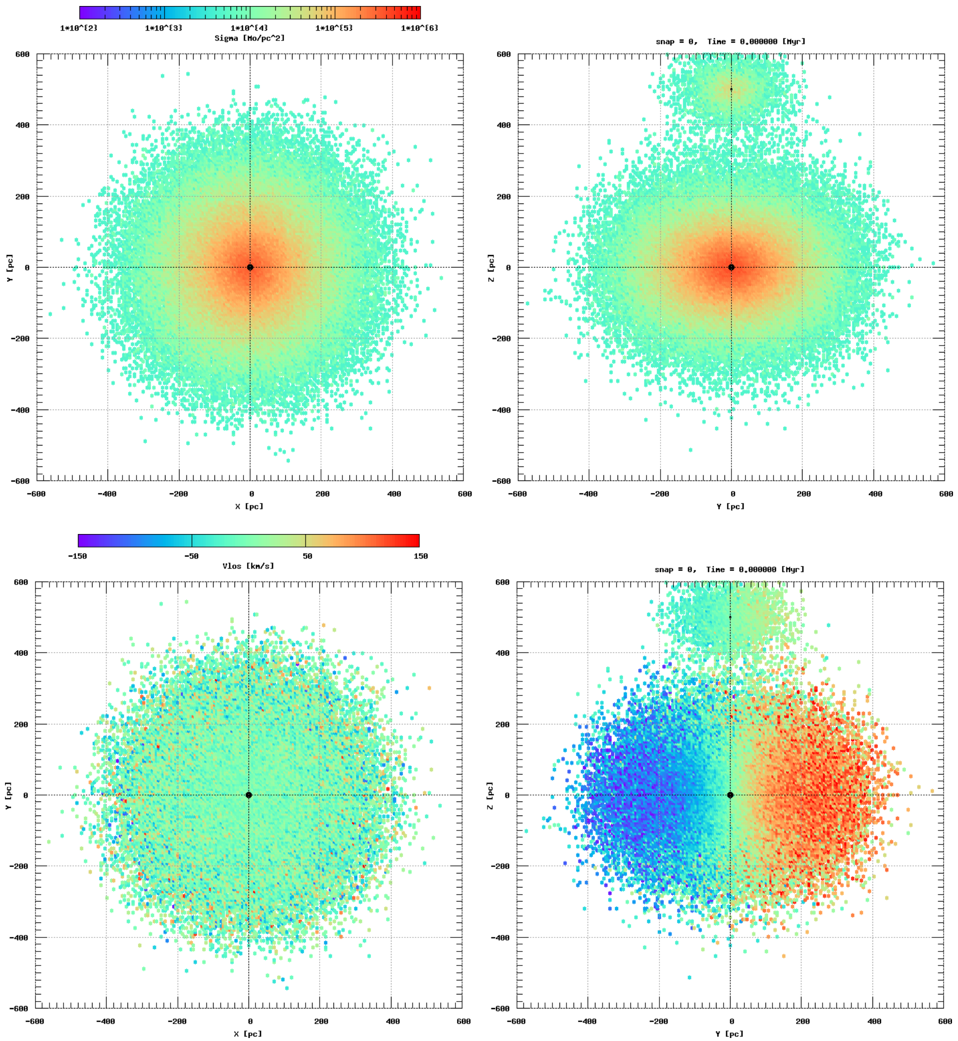

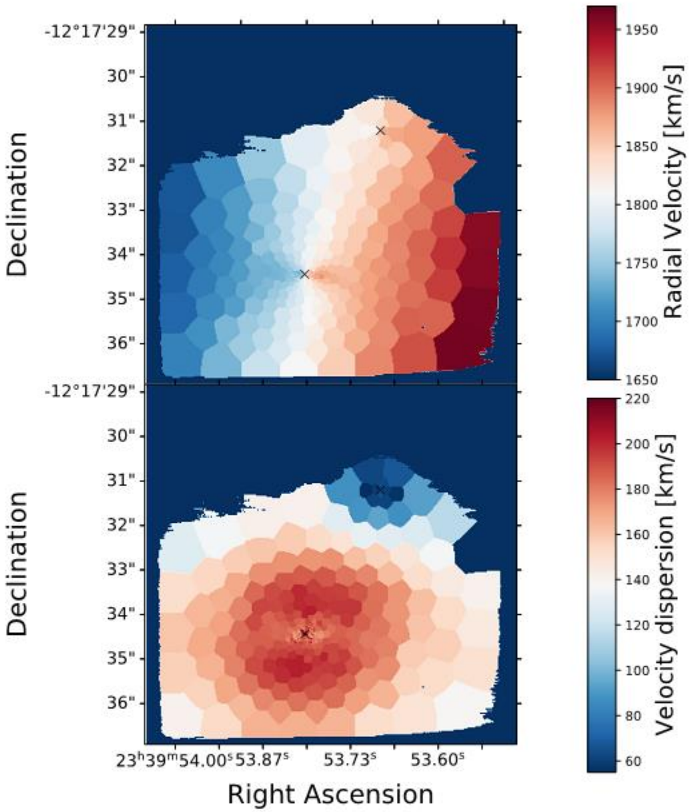

Fig. 2. *Top panel*: stellar velocities are shown across the binned MUSE cube. Regions without sufficient S/N were excluded from the fits. *Bottom panel*: stellar dispersion. Both panels have the data in spatial bins of at least $S/N = 25$, and the two Nuclei are marked with a black x.

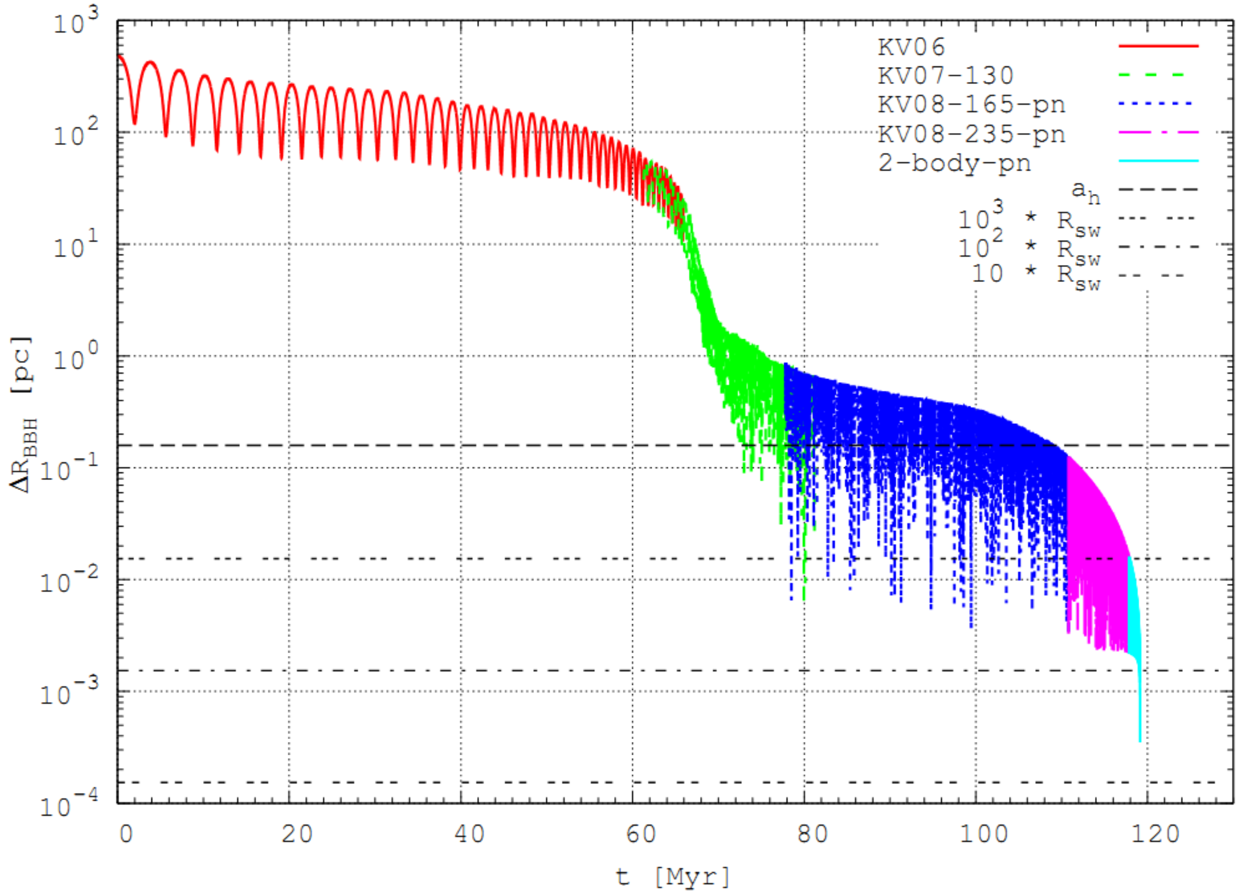

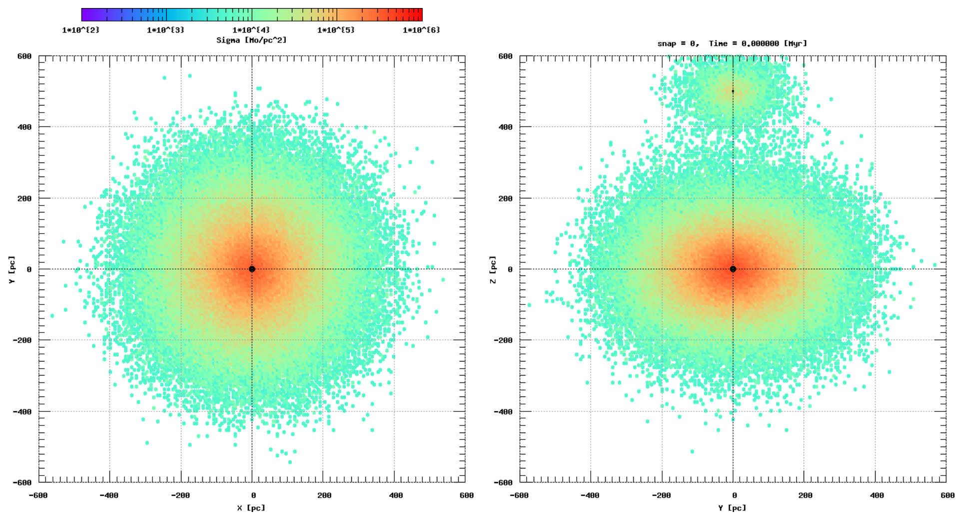

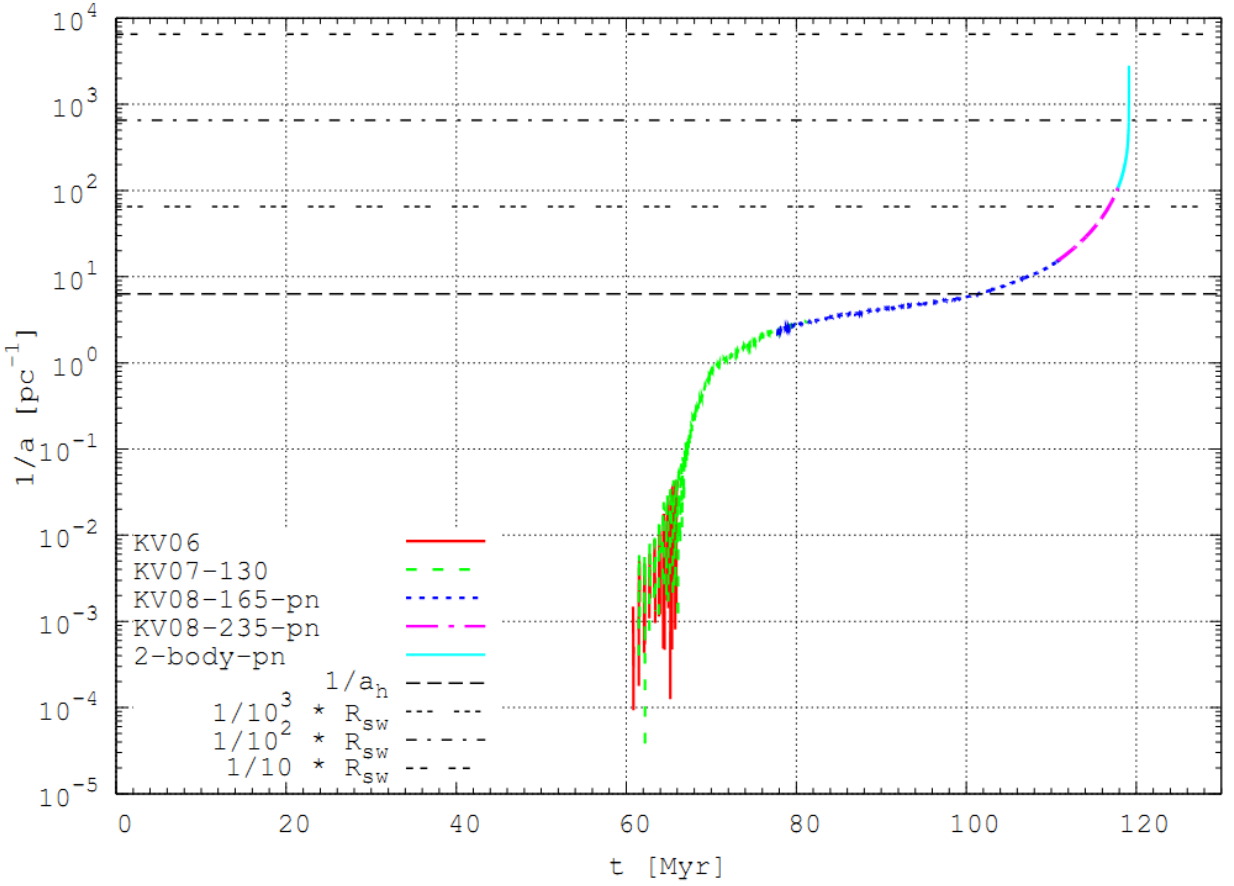

N = 0.3M; N = 0.6M; N = 1.0M; …x2 .

M_NB = 1.0E+09 [Mo] R_NB = 100 [pc]
V_NB = 207.3865 [km/s] T_NB = 0.4715 [Myr]
c = 1445.5734 [NB]

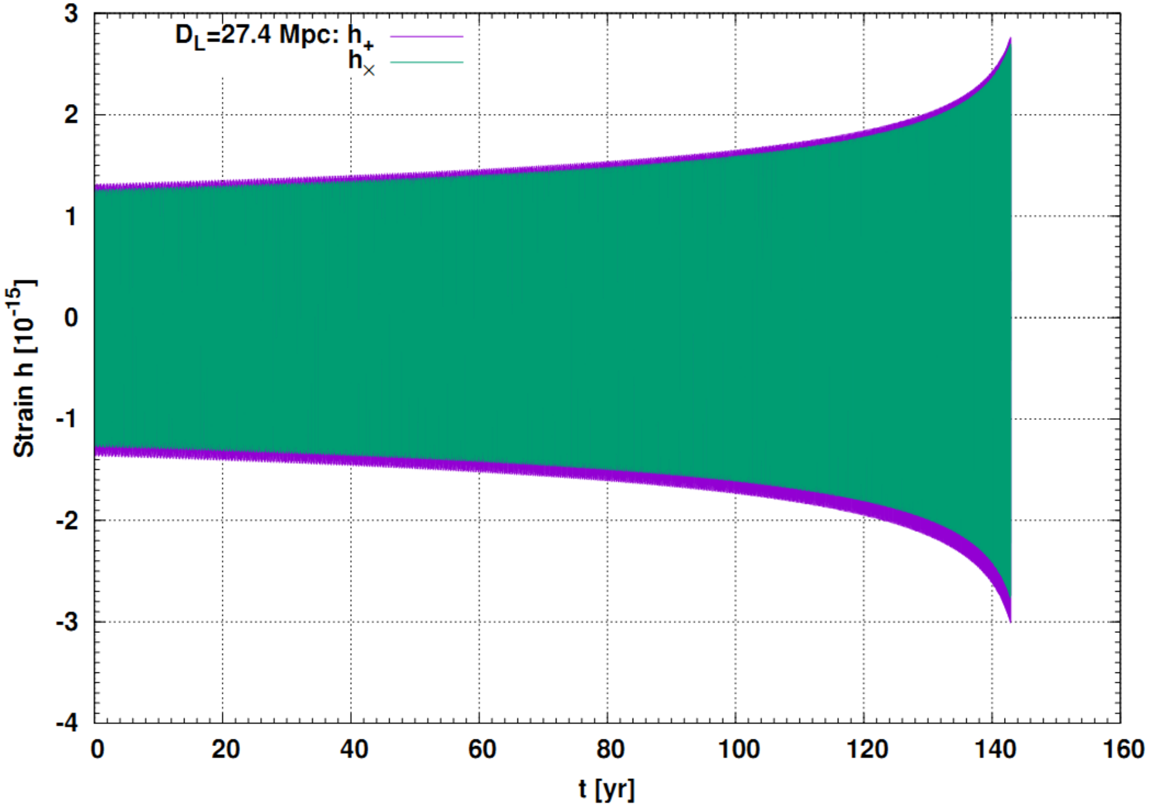

D_L=27.4 Mpc: h_+
h_×
Strain h [10^-15]
t [yr]

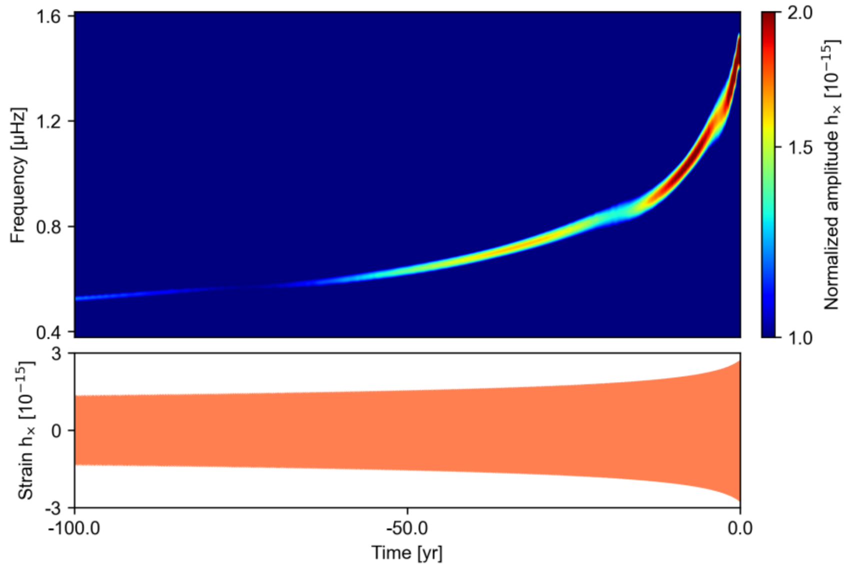

Frequency [μHz]
Normalized amplitude h_× [10^−15]
Strain h_× [10^−15]
Time [yr]

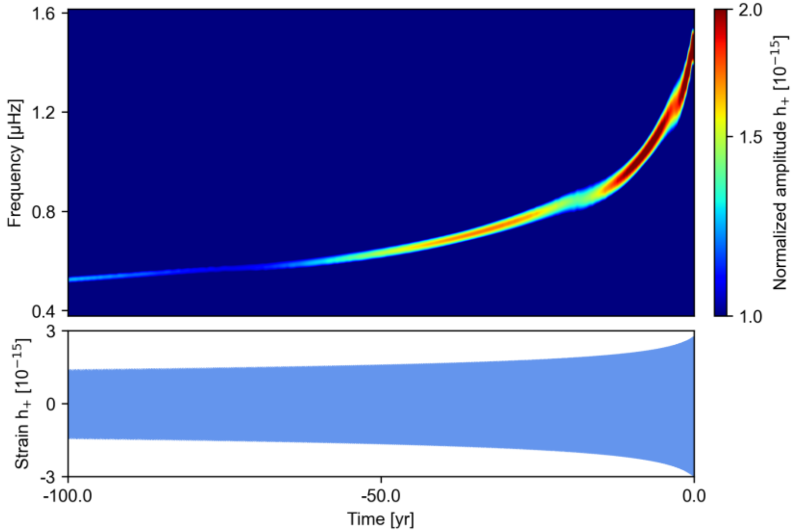

Frequency [μHz]
Normalized amplitude h_+ [10^−15]
Strain h_+ [10^−15]
Time [yr]

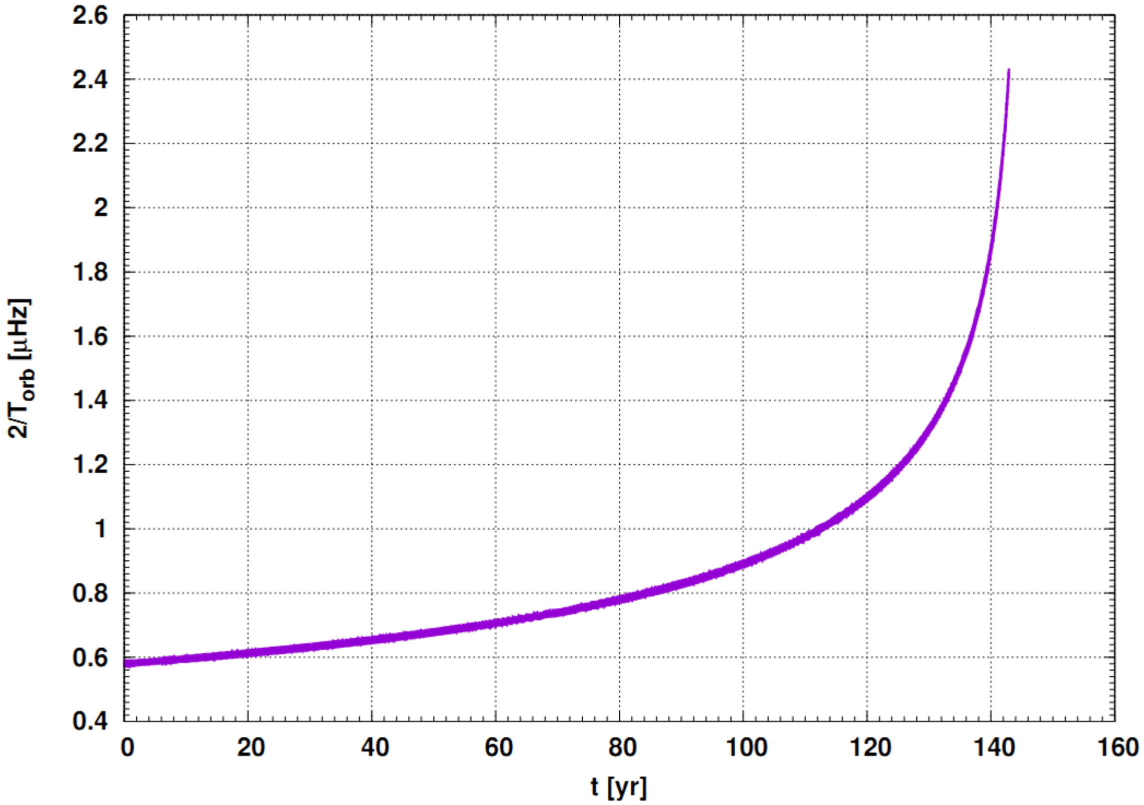

2/T_orb [μHz]
t [yr]

Thank you for your attention…

☺